

1 **Molecular Landscape of Anti-Drug Antibodies Reveals the Mechanism of the Immune**
2 **Response Following Treatment with TNF α Antagonists**

3 *Running title: Molecular landscape of anti-drug antibodies*

4 ^{1,†}Anna Vaisman-Mentesh, ^{1,†}Shai Rosenstein, ²Miri Yavzori, ¹Yael Dror, ²Ella Fudim,
5 ²Bella Ungar, ²Uri Kopylov, ²Orit Picard, ¹Aya Kigel, ²Shomron Ben-Horin, ¹Itai Benhar,
6 ^{1,*}Yariv Wine

7
8 ¹George S. Wise Faculty of Life Sciences, School of Molecular Cell Biology and Biotechnology,
9 Tel Aviv University, Ramat Aviv, Israel

10 ²Gastroenterology Department, Sheba Medical Center and Sackler School of Medicine, Tel-Aviv
11 University, Tel Hashomer, Israel

12 [†] These authors have contributed equally to this work.

13 *Author for correspondence: Yariv Wine

14 yarivwine@tauex.tau.ac.il

15

16 **Keywords:** Immunogenicity, anti-drug antibodies, next generation sequencing, Ig-Seq, BCR-Seq,
17 immune repertoire, antibody repertoire, proteomics, high-throughput sequencing, monoclonal
18 antibody, biologics, therapeutic antibodies

19

20 **Abstract**

21

22 Drugs formulated from monoclonal antibodies (mAbs) are clinically effective in various diseases.

23 Repeated administration of mAbs, however, elicits an immune response in the form of anti-drug-

24 antibodies (ADA), thereby reducing the drug's efficacy. Notwithstanding their importance, the

25 molecular landscape of ADA and the mechanisms involved in their formation are not fully

26 understood. Using a newly developed quantitative bio-immunoassay, we found that ADA

27 concentrations specific to TNF α antagonists can exceed extreme concentrations of 1 mg/ml with

28 a wide range of neutralization capacity. Our data further suggest a preferential use of the λ light

29 chain in a subset of neutralizing ADA. Moreover, we show that administration of TNF α

30 antagonists result in a vaccine-like response whereby ADA formation is governed by the

31 extrafollicular T cell-independent immune response. Our bio-immunoassay coupled with insights

32 on the nature of the immune response can be leveraged to improve mAb immunogenicity

33 assessment and facilitate improvement in therapeutic intervention strategies.

34

35

36 **MAIN TEXT**

37

38 **Introduction**

39 More than 30 years since the approval of the first therapeutic monoclonal antibody (mAb) for
40 clinical use, the therapeutic mAb market has expanded exponentially, establishing mAbs as one of
41 the leading biopharmaceutical therapeutic modalities (1). Although mAbs hold significant
42 promise for improving human health, their repeated administration is often highly immunogenic
43 and can elicit an undesirable anti-drug antibody (ADA) response (2). The formation of an ADA
44 response interferes with the effect of the drug or neutralizes it thereby altering the drug's
45 pharmacokinetic (PK) and pharmacodynamic (PD) properties and reducing its efficacy (3), and
46 eventually may lead to a severe adverse immune reaction in humans (4).

47 Immunogenicity of mAbs and the formation of an ADA response has been suggested to be
48 dependent on the interplay between factors related to the drug itself (e.g., non-human sequence,
49 glycosylation, impurities, aggregation), to the patient (e.g., disease type, genetic factors,
50 concomitant immunomodulators), or to the drug's route and frequency of administration (5, 6).
51 However, the molecular mechanisms that lead to the induction of ADA are not well understood
52 and were initially thought to be related to the murine origin of the mAbs because they were
53 recognized as "non-self" by the human immune system. This idea propelled the mAb discovery
54 field to focus on engineering refined mAbs by reducing the nonhuman portions and developing
55 chimeric, humanized, and fully human mAbs by using human libraries or humanized mice at the
56 mAb discovery phase (7).

57 Unfortunately, this strategy did not abolish the immunogenicity potential of mAbs and the
58 associated induction of ADA. The question of why and how ADA develop is further complicated
59 by data indicating that some patients develop ADA, and some do not, and by the observation that
60 the extent of immunogenicity may differ among patients receiving the same mAb (8). ADA that
61 develop in patients treated with an mAb can be stratified into two main categories: 1) neutralizing
62 ADA (*nt*ADA) that directly block and interfere with the drug's ability to bind its target, and 2)
63 non-neutralizing ADA (i.e., binding ADA *b*ADA) that recognize other epitopes on the drug while
64 still retaining the mAb binding activity (9). *nt*ADA are generally considered to be more important
65 in the clinical setting than *b*ADA because they directly reduce a drug's efficacy. However, *b*ADA
66 may indirectly reduce the therapeutic efficacy of an mAb by compromising bioavailability or

67 accelerating drug clearance from the circulation. In both cases, *nt*ADA and *b*ADA substantially
68 alter the PK and PD of the mAb being administered (10).

69 Originator and biosimilar tumor necrosis factor alpha (TNF α) antagonistic mAbs are used
70 extensively in clinical settings to treat inflammatory bowel disease (IBD; e.g., Crohn's disease
71 and ulcerative colitis), rheumatoid arthritis, and other chronic inflammatory associated disorders
72 such as psoriasis, psoriatic arthritis, and ankylosing spondylitis (11). TNF α antagonists help
73 reduce inflammatory responses by targeting both membrane-bound and soluble TNF α .
74 Neutralizing soluble TNF α prevents its binding to its receptor and impedes the secretion and
75 upregulation of the signal cascade, thereby inhibiting its biological activity. The binding of TNF α
76 antagonists to transmembrane TNF α on immune effector cells causes their destruction by
77 inducing cell apoptosis or cell lysis through reverse signaling (12).

78 Currently, five TNF α antagonists have been approved by both the U.S. Food and Drug
79 Administration and the European Medicines Agency: infliximab (IFX), adalimumab (ADL),
80 etanercept, golimumab, and certolizumab pegol (2). Additionally, several biosimilars have
81 already been approved or are in various stages of development (13). Both IFX and ADL belong to
82 the group of TNF α antagonists and are routinely used in clinical settings to treat inflammatory
83 diseases. IFX is a chimeric mAb (75% human and 25% murine), whereas ADL is fully human.
84 The reported immunogenicity extent of these drugs is inconsistent. Whereas pharmaceutical
85 companies report 10–15% and 2.6–26% immunogenicity for IFX and ADL, respectively (14),
86 clinical data suggest higher immunogenicity rates for these drugs (15). Patients treated with IFX
87 and ADL can be stratified based on the characteristics of their response to treatment or lack
88 thereof. Primary non-responders are patients whose disease does not respond to the drug at all,
89 and a certain subset of these may be mediated via early formation of ADA (15, 16). Secondary
90 non-responders are patients who initially respond to the drug but later fail treatment, often due to
91 development of ADA (for IFX, this was reported to develop mostly within 12 months of
92 treatment initiation) (16).

93 Studies reporting immunogenicity following mAb administration and ADA prevalence have been
94 inconsistent due in part to the various assay formats used to monitor immunogenicity in the clinic
95 (17). Current limitations of each available format might reduce utility in clinical and research
96 settings and complicate data interpretation. Some assays have a poor dynamic range and may
97 generate false negative results because of interfering interaction with another circulating drug, or
98 conversely, false positive results due to the presence of other antibodies such as rheumatoid factor

99 (18). The pros and cons of available ADA detection assays were previously elaborated, and the
100 formation of ADA following treatment with IFX, ADL, and other TNF α antagonists, including
101 newly developed biosimilars, have been extensively studied and reviewed elsewhere (5, 19-21).
102 Notwithstanding the effort invested in understanding the reasons that mAb immunogenicity and
103 strategies to increase mAb efficacy, little is known about the molecular mechanism that governs
104 the formation of ADA following treatment with an mAb.

105
106 In this study, we investigated the molecular landscape of ADA following treatment with
107 TNF α antagonists. First, we developed a simple bio-immunoassay that accurately quantifies ADA
108 levels in patient sera. We further modified the bio-immunoassay to evaluate the neutralization
109 capacity of the ADA. Next, we aimed to profile the immune response following mAb
110 administration. We used flow cytometry to determine the frequency of B cells in the circulation
111 and whether the dynamics of the immune response was akin to vaccine response. Finally, we used
112 next-generation sequencing (NGS) and high-resolution shotgun tandem mass spectrometry (LC-
113 MS/MS) to elucidate the molecular composition of serum ADA. Using our bio-immunoassay we
114 found that ADA levels in sera from 54 patients ranged between 2.7 and 1,268.5 $\mu\text{g/ml}$. The
115 modified bio-immunoassay enabled us to differentiate between patients who have high and low
116 neutralization capacity. Interestingly, we found that patients with a high neutralization capacity
117 showed a strong bias in the λ/κ light chain ratio thereby suggesting that *nt*ADA exhibits a
118 preference for λ light chains.

119 To elucidate the nature of the immune response following drug administration we chose to study a
120 patient with IBD who was treated with IFX and who had high ADA levels and neutralization
121 capacity. At 10 days (D10) following IFX infusion, the patient exhibited an approximately 13-
122 fold increase in the frequency of plasmablasts (PB) and unchanged frequency of activated
123 memory B cells (mBC), compared with the pre-infusion time point (D0). Comparative NGS
124 analysis of the antibody heavy chain variable region (V_H) from isolated PB at D0 and D10,
125 showed a significant temporal decrease in the level of somatic hypermutation (SHM) and an
126 increase in the length of the complementary determining region 3 of the antibody heavy chain
127 (CDRH3). Moreover, the proteomic analysis of serum ADA supports the observation obtained
128 from the neutralization capacity assays, that a preference for using λ light chains exists. These
129 data suggest a possible mechanism whereby the humoral immune response following the
130 administration TNF α antagonists is governed by a T cell-independent (TI) response. This
131 response may be induced by the formation of immunocomplexes (drug-TNF α -ADA) serving as a

132 strong driver of immunogenicity that in-turn diverts the immune response to TI pathway were B
133 cells are activated by B cell receptor (BCR) cross-linking.

134 **Materials and Methods**

135 **Over expression and purification of rhTNF α**

136 The sequence-encoding residues Val77–Leu233 of human TNF α was cloned and fused to the N-
137 terminal 6xHis tag in pET-28a+ vector (Novagen) and transformed into *Escherichia coli* Rosetta
138 (DE3) cells (Novagen). A single colony was inoculated into 2ml LB supplemented with
139 Kanamycin at final concentration of 100 μ g/ml and incubated over night (O.N.) at 37°C, 250
140 RPM. The culture was next re-inoculated into a 0.5L Erlenmeyer containing LB supplemented
141 with Kanamycin, and grown at 37°C 250RPM until O.D.₆₀₀~0.6-0.8 was reached. Induction was
142 carried out by supplementing bacterial culture with IPTG (0.1mM final concentration) and
143 incubating the culture for 3 hours at 37°C, 250RPM. Bacterial cells were harvested by
144 centrifugation at 8000 RPM, 15 minutes, at 10°C (SORVALL RC6 Plus, Thermo Fisher
145 Scientific) and cell pellet was stored O.N. at -20°C. Next, pellet was re-suspended in 30ml of
146 binding buffer (50mM sodium phosphate buffer pH 8.0, 300mM NaCl, 10mM imidazole) and
147 sonicated on ice for 8 cycles of 30 seconds pulse with 2-minute pause (W-385 sonicator, Heat
148 Systems Ultrasonics). Following sonication, cells were centrifuged at 12000 RPM, 30 minutes,
149 4°C (SORVALL RC 6+) and supernatant was applied to a HisTrap affinity column (GE
150 Healthcare) that was pre-equilibrated with binding buffer. All affinity purification steps were
151 carried out by connecting the affinity column to a peristaltic pump with flow rate of 1/ml/min.
152 Column was washed with 5 column volumes (CV) of wash buffer (50mM Sodium phosphate, pH
153 8.0, 300mM NaCl, 10% glycerol, 20mM imidazole) followed by elution of rhTNF α with 5CV of
154 elution buffer (50mM Sodium phosphate, pH 6.0, 300mM NaCl, 10% glycerol, 500mM
155 imidazole). Elution was collected in 1ml fractions and were analyzed by 12% SDS–PAGE.
156 Fractions containing clean rhTNF α were merged and dialyzed using Amicon Ultra (Mercury)
157 cutoff 3K against PBS (pH 7.4). Dialysis products were analyzed by 12% SDS–PAGE for purity
158 and concentration was measured using Take-5 (BioTek Instruments). To test functionality of the
159 produced rhTNF α , 96 well plate (Nunc MaxiSorp™ flat-bottom, Thermo Fisher Scientific) was
160 coated with 1 μ g/ml (in PBS) of purified rhTNF α and commercial hTNF α (PHC3011, Thermo
161 Fisher Scientific) and incubated at 4°C O.N. ELISA plates were then washed three times with
162 PBST (0.1% v/v Tween 20 in PBS) and blocked with 300 μ l of 2% w/v BSA in PBS for 1 hour at
163 37°C. Next, ELISA plates were washed three time with PBST, and incubated for 1 hour, room

164 temperature (RT) in triplicates with anti-TNF α mAb (Infliximab or Adalimumab) in 2% w/v
165 BSA, PBS at the starting concentration of 50nM with 3-fold dilution series. Plates were then
166 washed three times with PBST with 30 second incubation time at each washing cycle. For
167 detection, 50 μ l of anti-human H+L HRP conjugated antibody (Jackson) was added to each well
168 (1:5000 ratio in 2% w/v BSA in PBS) and incubated for 1 hour at RT, followed by three washing
169 cycles with PBST. Developing was carried out by adding 50 μ l of 3,3',5,5'-Tetramethylbenzidine
170 (TMB, Southern Biotech) and reaction was quenched by adding 50 μ l 0.1M sulfuric acid. Plates
171 were read using the Epoch Microplate Spectrophotometer ELISA plate reader (BioTek
172 Instruments).

173 **Over expression and purification of IdeS**

174 The coding sequence corresponding to amino acid residues 38–339 of *S. pyogenes* IdeS
175 (numbered from the start of the signal sequence) was sub-cloned into the expression vector
176 pET28b (Novagen). The coding sequencing was sub-cloned at the 3' end of Thioredoxin 6xHis-
177 TEV. The complete construct was sub-cloned as previously described (22) and was kindly
178 donated by Dr. Ulrich von Pawel-Rammingen from the Department of Molecular Biology, Umea
179 University. The transformation of pET-TRX_b plasmid harboring the IdeS encoding gene (pET-
180 IdeS) was carried out as follows: 200 μ l of chemical-competent *E. coli* BL21-DE3 cells were
181 thawed on ice for 20 minutes. 50ng of the plasmid pET-IdeS was added to the thawed competent
182 cells and incubated on ice for 20 minutes with gentle mixing every 5 minutes. Next, heat shock
183 was applied by incubating the cells at 42°C for 2 minutes followed by incubation on ice water for
184 2 minutes. For phenotypic expression, 800 μ l of LB was added, and cells were incubated at 37°C,
185 250 RPM for 1 hour in a horizontal position. Cells were plated on LB agar supplemented with
186 Kanamycin and incubated at 37°C overnight (O.N). Single colony was inoculated into 2ml LB
187 supplemented with Kanamycin and incubated O.N. at 37°C, 250 RPM. Next day, 2ml from the
188 grown cultures were inoculated into two 2liter flasks, each containing each 500ml LB
189 supplemented with Kanamycin. Over expression and purification of IdeS was carried out as
190 described for rhTNF α with a minor modification as follow: Ides was eluted with imidazole
191 gradient (50, 150, 500mM imidazole), total of 20ml. 20 fractions of 1ml were collected from each
192 elution step and evaluated for their purity using 12% SDS–PAGE. All fractions containing clean
193 IdeS were merged and dialyzed O.N. at 4°C against 4L of PBS (pH 7.4), using SnakeSkin dialysis
194 tubing with 10 kDa cutoff (Thermo Fisher Scientific). Dialysis products were analyzed by 12%
195 SDS–PAGE.

196 **Production of mAb-F(ab')₂**

197 Intact clinical grade IFX or ADL (designated here as mAb) were digested using in-house
198 produced IdeS. 10mg of mAb was incubated with 300µg of IdeS in the final volume of 500µl
199 PBS for 2.5 hours at 37⁰C, followed by a spike-in of additional 300µg of IdeS to achieve full
200 digestion of the Fc fragments. IdeS inactivation was carried out by adding 0.1M of citric acid pH
201 3 and incubation for 1 minute at RT followed by the addition of PBS (pH 7.4) to neutralized
202 acidic pH. Next, reaction mixture was applied to a 1 mL HiTrap KappaSelect affinity column (GE
203 Healthcare Life Sciences). All affinity purification steps were carried out by connecting the
204 affinity column to a peristaltic pump with flow rate of 1ml/min. The reaction mixture was
205 recycled three times through the KappaSelect column to maximize the capture of intact mAb and
206 mAb-F(ab')₂. KappaSelect column was subsequently washed with 5CV of PBS and eluted with
207 10CV of 100mM glycine·HCl (pH 2.7). Collected 1ml elution fractions were immediately
208 neutralized with 100µl of 1.5M Tris·HCl (pH 8.8). Next, the recovered intact mAb and mAb-
209 F(ab')₂ fragments were applied to a custom packed 1ml Protein-G agarose column (GenScript).
210 The reaction mixture was recycled three times through the column, which was subsequently
211 washed with 5CV of PBS and eluted with 10CV of 100mM glycine·HCl (pH 2.7). The 10ml
212 elution fraction was immediately neutralized with 1ml of 1.5M Tris·HCl (pH 8.8). The recovered
213 10ml mAb-F(ab')₂ fragments were dialyzed overnight at 4°C against 4L of PBS (pH 7.4) using
214 SnakeSkin dialysis tubing with 10kDa cutoff (Thermo Fisher Scientific). Recovered mAb-F(ab')₂
215 sample were evaluated for purity by SDS-PAGE and their concentration measured by Take5
216 (BioTek instruments).

217 To test the functionality of the produced mAb-F(ab')₂, 96 ELISA plates (Nunc MaxiSorp™ flat-
218 bottom, Thermo Fisher Scientific) were coated with 1µg/ml of rhTNFα in PBS and incubated at
219 4°C O.N. ELISA plates were then washed three times with PBST and blocked with 300µl of 2%
220 w/v BSA in PBS for 1 hour at 37°C. Next, 50nM of intact mAb and mAb-F(ab')₂ (IFX or ADL)
221 in blocking solution was added to each well in triplicates in a 3 fold dilution series, and plates
222 were incubated at RT for 1 hour. Next, plates were washed three times with PBST with 30 second
223 incubation time at each washing cycle. For detection, HRP conjugated anti-human kappa light
224 chain (Jackson) was added to each well (50µl, 1:5000 ratio in 2% w/v BSA in PBS) and incubated
225 for 1 hour at RT, followed by three washing cycles with PBST. Developing was carried out by
226 adding 50µl of TMB and reaction was quenched by adding 0.1M sulfuric acid. Plates were read
227 using the Epoch Microplate Spectrophotometer ELISA plate reader. To evaluate the purity of the

228 mAb-Fa(b')₂ samples (i.e. to make sure there are no traces of intact antibody or Fc fragment in the
229 sample) , 96 ELISA plate (Nunc MaxiSorp™ flat-bottom, Thermo Fisher Scientific) were coated
230 with 5µg/ml of intact mAb and mAb-F(ab')₂ in PBS and incubated at 4°C O.N. Next, plates were
231 washed three time with PBST and blocked with 300µl 2% w/v BSA in PBS for 1 hour at 37°C.
232 Next, plates were washed three times with 300 µl PBST, followed by the incubation with HRP
233 conjugated anti-human IgG Fc antibody (Jackson) diluted 1:5000 in PBST. Developing was
234 carried out by adding 50µl of TMB and reaction was quenched by adding 0.1M sulfuric acid.
235 Plates were read using the Epoch Microplate Spectrophotometer ELISA plate reader (BioTek
236 Instruments).

237 **Generation of ADA standard**

238 A pool of 17 ADA to IFX positive sera were collected at Sheba Medical Center, and passed
239 through a 2ml custom packed protein G agarose column (GenScript). The pooled sera was
240 recycled three times over the column, which was subsequently washed with 5CV of PBS and
241 eluted with 10CV of 100mM glycine·HCl (pH 2.7). The 10ml elution fraction was immediately
242 neutralized with 1ml of 1.5M Tris·HCl (pH 8.8). The purified mAbs were immediately passed
243 over a custom made rhTNFα affinity column (NHS-activated agarose beads, Thermo Fisher
244 Scientific) in gravity mode. The purified mAbs were recycled three times over the column, which
245 was subsequently washed with 5CV of PBS and eluted with 10CV of 100mM glycine·HCl (pH
246 2.7). The 10ml elution fraction was immediately neutralized with 1ml of 1.5M Tris·HCl (pH 8.8).
247 The purified mAbs were dialyzed overnight at 4°C against 4L of PBS (pH 7.4) using SnakeSkin
248 dialysis tubing with 10kDa cutoff (Thermo Fisher Scientific). Purified mAbs were analyzed for
249 purity using 12% SDS-PAGE and concentration was determined by Take3 (BioTek instruments).

250 To test functionality, 96 ELISA plate were coated with 5µg/ml of mAb-F(ab')₂ in PBS (pH 7.4)
251 and incubated at 4°C O.N. ELISA plates were then washed three times with PBST and blocked
252 with 300µl of 2% w/v BSA in PBS for 1 hour at 37°C. Next, 50nM of the purified ADA in
253 blocking solution were added to each well in triplicates with 3-fold dilution series and plates were
254 incubated at RT for 1 hour. Next, plates were washed three times with PBST with 30 second
255 incubation time at each washing cycle. Next, anti-human Fc HRP conjugate (Jackson) was added
256 to each well at the detection phase (50µl, 1:5000 ratio in 2% w/v BSA in PBS) and incubated for
257 1 hour at RT, followed by three washing cycles with PBST. Developing was carried out by
258 adding 50µl of TMB and reaction was quenched by adding 0.1M sulfuric acid. Plates were read
259 using the Epoch Microplate Spectrophotometer ELISA plate reader.

260 **Quantitative measurement of ADA in serum**

261 The schematic configuration of the bio-immunoassay for the quantitative measurement of ADA in
262 serum is described in Fig. 3B and was carried out as follows: ELISA plates that were coated
263 overnight at 4°C with 5µg/ml produced IFX-F(ab')₂ in PBS (pH 7.4). ELISA plates were then
264 washed three times with PBST and blocked with 300µl of 2% w/v BSA in PBS for 1 hour at
265 37°C. Next, triplicates of 1:400 diluted serum samples were added at triplicates and serially
266 diluted 2 fold in 2% w/v BSA in PBS, 10% horse serum (Biological Industries) and 1% Tween 20
267 in PBS (1:400– 1:51,200 serum dilution factor). Plates were incubated for 1 hour at RT. On the
268 same plate, serial dilutions of 10nM ADA standard were incubated in triplicate and serially
269 diluted 2 fold in 2% w/v BSA in PBS, 10% horse serum (Biological Industries) and 1% Tween 20
270 in PBS, to allow the conversion of the tested serum to units per milliliter. ELISA plates were
271 washed three times with PBST and 50µl of HRP conjugated anti-human IgG Fc was added to
272 each well (50µl, 1:5000 ratio in 2% w/v BSA in PBS) and incubated for 1 hour at RT. ELISA
273 plate was then washed three times with PBST and developed by adding 50µl of TMB followed by
274 quenching with 50µl 0.1M sulfuric acid. Plates were read using the Epoch Microplate
275 Spectrophotometer ELISA plate reader.

276 **Neutralization index of ADA**

277 Neutralization capacity was determined using ELISA plates that were coated overnight at 4°C
278 with 5µg/ml IFX-F(ab')₂ in PBS (pH 7.4). Next, coating solution was discarded and ELISA plates
279 were blocked with 300µl of 2% w/v BSA in PBS for 1 hour at 37°C. Blocking solution was
280 discarded and 50µl of 200 nM rhTNFα in 2% w/v BSA were added to the positive rhTNFα wells,
281 and 2% w/v BSA in PBS was added to the negative rhTNFα wells for 1 hour at RT. Next,
282 triplicates of 1:400 diluted serum samples with/without 200nM rhTNFα were added to the
283 positive/negative rhTNFα wells (respectively) and serially diluted 2-fold in 2% w/v BSA, 10%
284 horse serum (Biological Industries) and 1% Tween 20 in PBS (1:400– 1:51,200 serum dilution
285 factor). Plates were incubated for 1 hour at RT. ELISA plates were washed three times with PBST
286 and 50µl of HRP conjugated anti-human IgG Fc antibody or anti HRP conjugated His-tag
287 antibody were added at the detection phase (50µl, 1:5000 ratio in 2% w/v BSA in PBS) and
288 incubated for 1 hour at RT, followed by three washing cycles with PBST. Developing was carried
289 out by adding 50µl of TMB and reaction was quenched by adding 0.1M sulfuric acid. Plates were
290 read using the Epoch Microplate Spectrophotometer ELISA plate reader.

291 Neutralization index was calculated as following: an ELISA equation curve was calculated
292 separately for wells with and without rhTNF α , using the GraphPad Prism software. The average
293 triplicate signal which are 3 x standard deviation above the background signal was substituted in
294 the ELISA equation curve to extract the serial dilution value. The logarithmic difference of the
295 value with/without rhTNF α represents the neutralization index.

296 **Blood processing**

297 IFX treated patients with IBD cared for in the Department of Gastroenterology at the Sheba
298 medical center were included in the study. All subjects signed an informed consent, and the study
299 was approved by the Ethics Committee of the medical center. All patients received IFX on a
300 scheduled regimen and blood samples were drawn immediately before their scheduled IFX
301 infusion. Blood was collected into a single Vacutainer Lithium Heparin collection tube (BD
302 Bioscience).

303 For NGS analysis, blood was collected from a male donor treated with IFX, before IFX
304 administration and 10 days after administration. 30ml of peripheral blood were collected into 3
305 single Vacutainer K-EDTA collection tubes (BD Biosciences). Collection of peripheral blood
306 mono-nuclear cells (PBMCs) was performed by density gradient centrifugation, using Uni-
307 SepMAXI+ lymphocyte separation tubes (Novamed) according to the manufacturer's protocol.

308 **Fluorescence-Activated Cell Sorting Analysis and sorting of B cell populations**

309 PBMCs were stained for 15 minutes in cell staining buffer (BioLegend) at RT in the dark using
310 the following antibodies: anti-CD3-PerCP (clone OKT3; BioLegend), anti-CD19- Brilliant
311 Violet 510 (clone HIB19; BioLegend), anti-CD27-APC (clone O323; BioLegend), anti-CD38-
312 APC-Cy7 (clone HB-7; BioLegend), and anti-CD20-FITC (clone 2H7; BioLegend).

313 The following B cell population was sorted using a FACS Aria cell sorter (BD Bioscience):
314 CD3-CD19+CD20-CD27++CD38^{high}

315 B cell subpopulations were sorted and collected into TRI Reagent solution (Sigma Aldrich) and
316 frozen at -80°C.

317 **Amplification of V_H and V_L repertoires from B cells**

318 Total RNA was isolated using RNeasy micro Kit (Qiagen), according to manufacturer's protocol.
319 First-strand cDNA generation was performed with 100ng of isolated total RNA using a
320 SuperScript RT II kit (Invitrogen) and oligo-dT primer, according to manufacturer's protocol.
321 After cDNA synthesis, PCR amplification was performed to amplify the V_H and V_L genes using a
322 primer set described previously (23) with overhang nucleotides to facilitate Illumina adaptor
323 addition during the second PCR (Table S1). PCR reactions were carried out using FastStart™
324 High Fidelity PCR System (Roche) with the following cycling conditions: 95°C denaturation for
325 3 min; 95°C for 30 sec, 50°C for 30 sec, and 68°C for 1 min for four cycles; 95°C for 30 sec,
326 55°C for 30 sec, and 68°C for 1 min for four cycles; 95°C for 30 sec, 63°C for 30 sec, and 68°C
327 for 1 min for 20 cycles; and a final extension at 68°C for 7 min. PCR products were purified using
328 AMPure XP beads (Beckman Coulter), according to manufacturer's protocol (ratio x 1.8 in favor
329 of the beads). Recovered DNA products from the first PCR was applied to a second PCR
330 amplification to attach Illumina adaptors to the amplified V_H and V_L genes using the primer
331 extension method as described previously (24). PCR reactions were carried out using FastStart™
332 High Fidelity PCR System (Roche) with the following cycling conditions: 95°C denaturation for
333 3 min; 95°C for 30 sec, 40°C for 30 sec, and 68°C for 1 min for two cycles; 95°C for 30 sec, 65°C
334 for 30 sec, and 68°C for 1 min for 7 cycles; and a final extension at 68°C for 7 min. PCR products
335 were applied to 1% agarose DNA gel electrophoresis and gel-purified with Zymoclean™ Gel
336 DNA Recovery Kit (Zymo Research) according to the manufacturer's instructions. V_H and V_L
337 libraries concentration were measured using Qubit system (Thermo Fisher Scientific) and library
338 quality was assessed using the Bioanalyzer 2100 system (Agilent) or the 4200 TapeStation system
339 (Agilent). All V_H libraries were produced in duplicates starting with RNA as the common source
340 template. The V_L were produced with one replicate.

341 V_H and V_L libraries from sorted B cell were subjected to NGS on the MiSeq platform with the
342 reagent kit V3 2x300 bp paired-end (Illumina), using an input concentration of 16pM with 5%
343 PhiX.

344 Raw fastq files were processed using our recently reported ASAP webserver (25). ASAP analysis
345 resulted in a unique, full-length V_H and V_L gene sequences database for each time point. The
346 resultant database was used as a reference database to search the LC-MS/MS spectra.

347 **Proteomic Analysis of the Serum ADA to IFX**

348 Total IgG from each time point (D0, D10) were purified from 7-10ml of serum by protein G
349 enrichment. Serum was diluted 2 fold and passed through a 5ml Protein G agarose column
350 (GeneScript). The diluted serum was recycled three times over the column, which was
351 subsequently washed with 10CV of PBS and eluted with 7CV of 100mM glycine·HCl (pH 2.7). A
352 total of 35 fractions of 1ml were collected and immediately neutralized with 100 μ l of 1.5M
353 Tris·HCl (pH 8.8). All elution fractions were evaluated for their purity using 12% SDS-PAGE
354 and 11 purified 1 ml IgG fractions were combined and dialyzed overnight at 4°C against 4L of
355 PBS (pH 7.4) using SnakeSkin dialysis tubing with 1 kDa cutoff (Thermo Fisher Scientific).

356 Next, 9mg of total IgG were digested with 100 μ g of IdeS in the final volume of 2ml PBS for 5
357 hour at 37°C. IdeS inactivation was carried out by adding 0.1M of citric acid pH 3 and incubation
358 for 1 minute at RT followed by the addition of PBS (pH 7.4) to neutralize the low pH. Total
359 serum F(ab')₂ was then applied to a one ml custom made affinity column comprised of IFX-
360 F(ab')₂ coupled to NHS-activated agarose beads (Thermo Fisher Scientific). The purified serum
361 F(ab')₂ were recycled three times over the affinity column, which was subsequently washed with
362 5CV of PBS and eluted with 15CV of 100mM glycine·HCl (pH 2.7) and collected into
363 Maxymum Recovery Eppendorf (Axygen Scientific). A total of 30x0.5ml elution fractions and
364 1x50ml flow-through were immediately neutralized with 50 and 100 μ l (respectively) of 1.5M
365 Tris·HCl (pH 8.8). The purified antigen-specific F(ab')₂ were dialyzed overnight at 4°C against
366 4L of PBS (pH 7.4) using SnakeSkin dialysis tubing with 10kDa cutoff (Thermo Fisher
367 Scientific). Elution and flow-through fractions were trypsin-digested, and resulting peptides were
368 fractionated and sequenced by nanoflow LC-electrospray MS/MS on an Orbitrap Velos Pro
369 hybrid mass spectrometer (Thermo Scientific), in the UT Austin mass spectrometry core facility
370 as described previously (26). MS/MS raw files were analyzed by MaxQuant software version
371 1.6.0.16 (27) using the MaxLFQ algorithm (28) and peptide lists were searched against the
372 common contaminants database by the Andromeda search engine (29) and a custom protein
373 sequence database consisting of the donor-specific V_H and V_L sequences derived from NGS of
374 individual donor B cells. All searches were carried out with cysteine carbamidomethylation as a
375 fixed modification and methionine oxidations as variable modifications. The false discovery rate
376 was set to 0.01 for peptides with a minimum length of seven amino acids and was determined by
377 searching a reverse decoy database. Enzyme specificity was set as C-terminal to arginine and
378 lysine as expected using trypsin as protease, and a maximum of two missed cleavages were
379 allowed in the database search. Peptide identification was performed with an allowed initial
380 precursor mass deviation up to 7ppm and an allowed fragment mass deviation of 20ppm. For LFQ

381 quantification the minimal ratio count was set to 2, and match between runs was performed with
382 three mass-spec injections originating from the same sample. MaxQuant output analysis file,
383 “peptides.txt”, was used for further processing. Total peptides that were identified in the elution
384 samples were filtered using the following criteria: (a) were not identified as contaminants; (b) did
385 not match to the reversed decoy database; (c) were identified as peptides derived from the region
386 comprising the CDRH3, J region, FR4 and the ASTK motif (derived from the N-terminal of the
387 C_{H1} region). The CDRH3 derived peptides were further characterized as informative CDRH3
388 peptides (*i*CDRH3 peptides) only if they map exclusively to a single antibody clonotype. A
389 clonotype was defined as all sequences that comprise CDRH3 with the same length and identity
390 tolerating one amino acid mismatch, and same V, J family. The intensities of high confidence
391 *i*CDRH3 peptides were averaged between replicates while including only peptides that were
392 observed in at least two out of the three replicates. Clonotype frequencies within each sample
393 were calculated using only *i*CDRH3 peptides and were determined to be antigen-specific if their
394 frequency in the elution fraction was at least 5 fold greater than their frequency in the flow-
395 through fraction. The CDRH3 sequences identified by the mapping of high confidence MS/MS
396 peptides were used to generate a complete list of full length VH sequences. These VH sequences
397 were used to analyze the repertoire measures of the antibodies that were identified in the donors’
398 serum.

399 Same filtering criteria was applied to peptides derived from the constant region of both κ and λ
400 light chains. By quantifying the accumulative intensities of these peptides, we calculated the ratio
401 of $\kappa:\lambda$ light chain from antibodies that were derived from the affinity column elution fraction
402 which represent both *nt*ADA and *b*ADA, and in the affinity column flow through fraction which
403 represent the depleted ADA fraction.

404 **Study population**

405 IFX and ADL treated patients with IBD cared for in the Departments of Gastroenterology at
406 Sheba medical center were included in the study. All subjects signed an informed consent, and the
407 study was approved by the Ethics Committee of Sheba medical center. IFX and ADL and ADA
408 serum levels were routinely measured at trough immediately before infusion. All patients received
409 IFX and ADL on a scheduled regimen. All patients that were included in this study exhibited low
410 through levels of IFX and ADL.

411

412 **Statistical analysis**

413 All curves were fitted on a sigmoidal dose–response curve and EC50 of each was calculated.
414 Mann-Whitney test was used to compare continuous variables. All reported P values were two-
415 tailed, and a P value less than 0.05 were considered statistically significant. All statistics were
416 performed with GraphPad Prism software (version 7, San Diego, California).

417 **Results**

418 **Production of mAb-F(ab')₂ to be used in the bio-immunoassay**

419 To investigate the molecular landscape of ADA following mAb administration we first aimed to
420 develop an accurate, sensitive, robust bio-immunoassay to determine ADA levels in sera. The
421 working hypothesis was that anti-idiotypic antibodies dominate the ADA compartment (21) thus,
422 the developed bio-immunoassay was based on the drugs' F(ab')₂ portion to be used as the antigen
423 (i.e. coating agent).

424 To achieve this, we used the immunoglobulin G (IgG)-cleaving enzyme (IdeS), a cysteine
425 proteinase enzyme that proteolytically cleaves immunoglobulins below the hinge region (30)
426 (Figure 1A). IFX was digested using IdeS by incubating 10 mg of clinical grade mAb with IdeS
427 to reach near complete digestion. Next, IFX-F(ab')₂ was purified from Fc regions and undigested
428 full IFX by consecutive affinity chromatography steps comprising protein A and kappaSelect
429 columns.

430 Recovered IFX-F(ab')₂ purity was evaluated by SDS-PAGE (Figure 1B) and ELISA (Figure 1C)
431 to ensure that the IFX-F(ab')₂ exhibits no traces of IFX-Fc/undigested IFX that will contribute to
432 the background level when using anti-Fc HRP conjugate at the detection phase. Recovered IFX-
433 F(ab')₂ samples were found to be highly pure with basal anti-Fc signal levels similar to the signal
434 observed in the control samples. The produced IFX-F(ab')₂ was tested for functionality by
435 measuring its TNF α binding capacity, using ELISA with TNF α as the coating agent, and was
436 found to show similar functionality as that of the intact IFX (Figure 1D). ADL was subjected to
437 the same preparative pipeline and demonstrated similar results (Figure S1).

438 **ADA Standard curve**

439 Quantification of total ADA in serum requires a standard reference. Thus, we generated a
440 standard ADA pool that facilitates the quantification of ADA levels in sera of patient treated with
441 IFX. ADA were pooled from several serum samples collected from patients treated with IFX and
442 purified by consecutive affinity chromatography steps comprising protein G and a custom-made
443 IFX-F(ab')₂ affinity columns. We confirmed the affinity enrichment of ADA by applying the
444 affinity chromatography elution fraction to ELISA with IFX-F(ab')₂ as the coated antigen (Figure
445 2A). The purity and concentration the recovered ADA were determined by SDS-PAGE (Figure
446 2B) and nanodrop.

447 Maximal serum concentration used in a bio-immunoassay (e.g. serum diluted 1:100 or 1:200) is a
448 major factor that may contribute to high background signal levels due to non-specific binding.
449 Screening several maximal serum dilutions showed that 1:400 initial serum dilution demonstrates
450 the lowest background signal (data not shown). To evaluate if serum will affect the signal
451 obtained from purified ADA, we spiked-in purified ADA into negative control serum that was
452 diluted 1:400 in PBS. Serial dilution of spiked-in ADA and purified ADA showed similar signal
453 in ELISA (Figure 2C) indicating that serum does not bias the ADA detection in our developed
454 bio-immunoassay.

455 **Quantitative measurement of ADA in serum**

456 ADA detection is technically challenging as both the analyte and antigen are antibodies which
457 may result in the inability to differentiate between the mAb and ADA. To overcome this
458 challenge, many assays were previously developed (5). One of these immunoassays is the anti-
459 human λ chain (AHLC) immunoassay that is used in clinical setups for monitoring the formation
460 of ADA (31). The principle of this assay is to detect ADA comprising λ light chain, thus avoiding
461 cross reactivity with the drug that comprises the κ light chain (Figure 3A).

462 While AHLC is suitable for monitoring the development of ADA in clinical setups, when one
463 aims to study the molecular composition of ADA there is a need to provide quantitative measures
464 of total ADA in serum. Thus, we developed a new bio-immunoassay based on the F(ab')₂ portion
465 of the mAb. The bio-immunoassay setup is described in Figure 3B and is based on mAb-F(ab')₂
466 as the coating antigen and anti-Fc HRP conjugate used as the detection antibody. Each of the
467 experimental setups to test ADA in serum included serum from a healthy donor as a control and
468 ADA standard for the quantitation of total ADA.

469 First, we applied the newly developed bio-immunoassay on two serum sample groups: one
470 negative and one positive for ADA as determined by the AHLC assay (AHLC⁽⁻⁾ and AHLC⁽⁺⁾,
471 respectively). We also included serum from a healthy subject to serve as a control for the assay
472 specificity (i.e. serum from a subject that was not exposed to IFX). As shown in Figure 3C-D, the
473 ELISA signals obtained when utilizing the new bio-immunoassay were higher compared to the
474 signal obtained with the AHLC assay. Moreover, applying the new bio-immunoassay on the
475 AHLC⁽⁻⁾ serum (no detected ADA with the AHLC assay) detected relatively high levels of ADA.
476 These results indicate that not all ADA were detected with the AHLC assay as this assay is based
477 on the detection of ADA that comprise the λ light chain only.

478 Next, to extend and generalize the above results, sera from 54 patients treated with IFX were
479 collected at the Chaim Sheba Medical Center and tested for drug levels and ADA using the
480 AHLC assay. The established cohort showed very low drug trough levels and based on the AHLC
481 results, sera were stratified into two groups: 25 serum samples were identified as AHLC⁽⁻⁾ and 29
482 as AHLC⁽⁺⁾. Using our newly developed quantitative bio-immunoassay, we found that ADA
483 levels in tested sera ranged between 1.82 to 1268.5 $\mu\text{g/ml}$. Serum ADA levels using AHLC
484 compared to the new bio-immunoassay are summarized in Table 1. More importantly, the new
485 bio-immunoassay demonstrated improved sensitivity compared to AHLC assay manifested in the
486 detection of higher concentrations of ADA in 46 out of the 54 serum samples, of which 17 out of
487 the 54 samples, belong to the AHLC⁽⁻⁾ group. Overall, the average fold increase in ADA detection
488 using the new bio-immunoassay compared to the AHLC assay was 14.13 and 53.26 for the
489 AHLC⁽⁺⁾ and AHLC⁽⁻⁾ groups, respectively.

490 **Neutralization index of ADA**

491 Due to high clinical relevance and different mechanism of action of *bADA* and *ntADA*,
492 identifying their relative abundances in serum can provide valuable insights regarding the nature
493 of the immune response following mAb administration. We therefore modified our newly
494 developed mAb-F(ab')₂ based bio-immunoassay by blocking the coated IFX-F(ab')₂ binding site
495 with TNF α in order to obtain a differential signal compared to the unblocked assay (Figure 4A).
496 In order to block the binding site of IFX-F(ab')₂ towards TNF α and prevent the binding of anti-
497 idiotypic ADA (i.e. *ntADA*) to the drug, recombinant human TNF α (rhTNF α) fused to a His-tag
498 was cloned and expressed (see materials and methods). In-house production of rhTNF α was
499 essential, as the N terminal His-tag was used for monitoring the presence of the rhTNF α
500 throughout the bio-immunoassay.

501 First, we evaluated the ability of rhTNF α to inhibit the binding of ADA to the coated IFX-F(ab')₂
502 by setting up a competitive ELISA where a series of ADA standard concentrations were
503 incubated with a series of fixed rhTNF α concentrations (data not shown). We observed a
504 competitive effect while rhTNF α was fixed at the concentration of 5nM (Figure 4B). This step
505 was important as it enabled us to determine the ADA equimolar concentration of rhTNF α to be
506 used that will fully occupy the IFX-F(ab')₂ binding site and will prevent the binding of *nt*ADA to
507 the coated (and blocked) IFX-F(ab')₂. We monitored the presence of rhTNF α using an HRP-
508 conjugated anti-His tag antibody and observed that if we aim to completely block ADA it is
509 required to use equimolar concentration of rhTNF α that corresponds to the highest
510 concentration of ADA in the assay (200nM).

511 In practice, IFX-F(ab')₂ binding site was blocked with rhTNF α by prior incubation of serum with
512 the coated IFX-F(ab')₂ hence, the differential signal w/ and w/o the presence of rhTNF α represent
513 the portion of ADA that could not bind the IFX-F(ab')₂ binding site thus, reflects the
514 neutralization capacity (hereby named neutralization index) of the ADA in the tested serum.
515 Using this assay, we evaluated the neutralization index of the 46 ADA positive sera from patients
516 treated with IFX and 7 ADA positive sera from patients treated with ADL. In sera from patients
517 treated with IFX, we noticed that there are two main neutralization index patterns: those with high
518 differential signal (Figure 5A) and low differential signal (Figure 5B). More interestingly, we
519 found that patients that were stratified as AHLC⁽⁺⁾ have a significantly higher neutralization index
520 compared to those that belong to the AHLC⁽⁻⁾ group (Figure 5C). This suggests that there is a
521 preferential usage of the λ light chain in *nt*ADA as the AHLC⁽⁺⁾ group is *a priori* defined by the
522 presence of ADA comprising the λ light chains. All sera from patients treated with ADL (n=7)
523 were subjected to modified bio-immunoassay and demonstrated high neutralization indexes
524 (Figure S2)

525 **IFX infusion induces a vaccine like immune response**

526 To further investigate the molecular landscape of ADA we explored the dynamics of the B cell
527 response following mAb administration. When investigating well-controlled clinical scenarios
528 such as samples obtained from post-vaccinated individuals, it is convenient to isolate the antigen-
529 specific B cell as they peak at a defined time window (23, 32). However, the characteristics of the
530 humoral response and ADA encoding B cell dynamics following mAb administration is unknown.
531 Our working hypothesis assumed that the immune response following mAb administration is a
532 vaccine-like response thus; we expected to observe a wave of PB peaking several days after IFX

533 infusion. It was previously demonstrated that boost vaccines induce a strong proliferation of PBs
534 and mBCs that can be detected in the blood circulation several days after the boost (33, 34). To
535 test if IFX administration induces a vaccine like response, we collected blood samples from a
536 patient that was found to be positive to ADA at two time points: prior to IFX infusion (D0) and 10
537 days after IFX infusion (D10). The second time point (D10) was determined in order to capture an
538 enriched population of antigen-specific PB as well as mBC that enable the establishment of a
539 donor-specific V_H database for the proteomic interpretation of peptides derived from ADA.

540 Peripheral blood mononuclear cells (PBMCs) were sorted by FACS and the frequency of PB
541 ($CD3^-CD19^+CD20^-CD27^{++}CD38^{++}$) and mBC ($CD3^-CD19^+CD20^+CD27^+$) subsets were
542 determined. We identified a 13-fold increase in the frequency of PB at D10 and no increase in the
543 mBC compartment. The PB data suggests that the B cell dynamics following IFX infusion
544 exhibits vaccine-like characteristics in accordance with our working hypothesis (Table 2, Figure
545 S3).

546 **Antibody repertoire of ADA encoding B-Cells**

547 The waves of PB following challenge is enriched with antigen-specific B cells (23, 32, 35). Based
548 on this, a major fraction of PB at D10 post mAb infusion is expected to comprise B cell clones
549 responding to the current antigen challenge. Thus, the repertoire of B cells at two time points
550 (pre- and post-infusion) is predicted to represent the overall differences in the ongoing ADA
551 encoding B cell response.

552 This diversity of antibodies is accomplished by several unique molecular mechanisms, including
553 chromosomal V(D)J rearrangement, somatic hypermutations (SHM) and class switch
554 recombination (25), processes that are mediated by recombination-activating gene (RAG) and
555 activation-induced cytidine deaminase (AID), respectively. The AID enzyme functions mainly in
556 secondary lymph nodes named germinal centers. Next-generation sequencing (NGS) of the
557 antibody variable regions (V-genes) coupled with advanced bioinformatics tools provides the
558 means to elucidate the antigen-specific antibody repertoire's immense diversity (36). To deep
559 sequences antibodies' V-genes, recovered RNA from sorted PB and mBC was used as the
560 template for first-strand cDNA synthesis, followed by PCR amplification steps to produce
561 barcoded amplicons of the V-genes of the antibody heavy chains (V_H) as described previously
562 (24). While NGS of antibodies is a powerful tool for immune repertoire analysis, relatively high
563 rates of errors accumulate during the experimental procedure. To overcome this challenge, we

564 generated duplicates of the antibody V-gene amplicons and sequenced them using the Illumina
565 MiSeq platform (2x300bp). The resultant V_H sequences were processed using our recently
566 reported ASAP webserver that was specifically developed to analyze NGS of antibody V-gene
567 sequences derived from replicates (25).

568 In our analysis, we concentrated on several repertoire measures that collectively provide a
569 molecular level characterization of the ADA: i) V(D)J family usage; ii) CDR3 length distribution;
570 iii) SHM levels, and, iv) isotype distribution. Our data revealed several interesting antibody
571 repertoire features that may shed light on the molecular mechanism involved in the formation of
572 ADA.

573 V(D)J gene family usage is stable

574 Examining the V(D)J family usage is important to determine whether the basal gene frequency is
575 similar to the expected frequency and if the B cell response following IFX infusion drives B cells
576 to exhibit a preferential V(D)J gene usage. Therefore, we examined the frequency of family usage
577 at two time points (D0 and D10), within PB and mBC subsets across isotypes (IgG and IgM).
578 The V(D)J family usage showed no marked difference between the two time points, B cell subsets
579 and isotypes. The frequency of V-gene family usage was also found to have similar frequency
580 profile as previously described (37, 38). For example, the V-gene family frequency showed that
581 the V3, V4 and V1 have the most prevalent representation followed by V2, V5 and V6 that had
582 significantly lower frequencies (Figure 6A). The same pattern trends were identified for the D and
583 J family usage.

584 CDRH3 length increases following IFX infusion

585 Composed of the V(D)J join with its inherent junctional diversity, the CDRH3 specifies the
586 antibody V_H clonotype. The V_H clonotype is an important immunological concept because it
587 accounts for antibodies that likely originate from a single B-cell lineage and may provide insight
588 on the evolution of the antigen-specific response (39). Here we defined V_H clonotype as the group
589 of V_H sequences that share germ-line V and J segments and have identical CDRH3 sequences. By
590 examining the length distribution of CDRH3 from PB across isotypes and time point we observed
591 a shift towards longer CDRH3 at D10 (Figure 7). Interestingly, this observation is in contrast to
592 previous studies that reported a decrease in the CDRH3 length post immunization with

593 pneumococcal (40) and hepatitis B vaccines (41) and when comparing antigen experienced B cell
594 to naïve B cells (42).

595 Somatic hypermutation levels decreases following IFX infusion

596 Examining the level of SHM following vaccination provides insights regarding the extent of the
597 affinity maturation that antigen-stimulated B cell undergo. It was previously reported that boost
598 vaccination induces a substantial increase of the SHM levels when comparing post- to pre-
599 vaccination (41). Despite the vaccine like response following IFX infusion, we observed in the
600 PB compartment a significant decrease in the SHM levels post-infusion, regardless if the
601 mutations were synonymous and non-synonymous (Figure 8).

602 **Proteomic analysis of ADA**

603 Analysis of serum antibodies provides a comprehensive profile of the humoral immune response
604 and is complementary to the transcriptomic analysis derived from NGS of the antibody V_H.
605 Applying an approach that integrates NGS and tandem mass spectrometry (LC-MS/MS) has been
606 shown to provide valuable data regarding the composition of antigen-specific serum antibodies
607 and their relationship to B cells and generates new insights regarding the development of the
608 humoral immune response in disease and following vaccination (23, 32). Here we utilized the
609 previously developed omics approach (26, 39) to elucidate the serum ADA composition following
610 IFX infusion. ADA from 10 ml of serum collected at D0 and D10 were subjected to protein G
611 affinity chromatography and total of 9 mg of recovered IgG was digested by IdeS to remove the
612 Fc regions that may mask the MS/MS signal obtained from low abundant peptides. Following 5
613 hours of digestion, the reaction mixture was subjected to custom made affinity column where the
614 IFX-F(ab')₂ was coupled to agarose beads and served as the antigen to isolate ADA. Recovered
615 48.57µg polyclonal ADA-F(ab')₂ (i.e., IFX-F(ab')₂-specific F(ab')₂) in the elution fraction and
616 total F(ab')₂ (depleted from ADA-F(ab')₂) in the flow through fraction were digested with trypsin
617 and injected to high-resolution tandem mass spectrometer analyzer in triplicates. LC-MS/MS raw
618 data files were analyzed using MaxQuant using label free quantitation mode (LFQ) and searched
619 against the custom antibody V-gene database derived from the NGS data of B cells isolated from
620 the same donor. Identified peptide from the interpretation of the proteomic spectra were stratified
621 into three types of peptides: informative peptides (*i*Peptide) that map uniquely to one antibody
622 clonotype in a region that is upstream to the CDRH3, non-informative CDRH3 peptides
623 (*ni*CDRH3) that map to the CDRH3 region of the antibody but do not map uniquely to a single

624 antibody clonotype and informative CDRH3 peptides (*i*CDRH3) that map uniquely to a single
625 antibody clonotype. Summary of identified peptides in LC-MS/MS are shown in Table 3. Beyond
626 the designation as *i*CDRH3 peptides, additional filtration steps were applied including peptides
627 that were present in more than 2 replicates, peptides in elution that show 5x fold frequency than in
628 the flow through. The *i*CDRH3 peptides enabled the identification of 62 unique ADA CDRH3
629 clonotypes with 205 associated full-length V-gene sequences. The resulting V-gene sequences
630 were analyzed to determine their V(D)J family usage and the B cell subset they are mapped to,
631 based on our NGS data (Figure 9).

632 The V(D)J family usage of the antibody variable region sequences that were identified by LC-
633 MS/MS (Figure 9A) showed a similar distribution as observed in the NGS data (Fig. 6A, Fig.
634 7A). V family frequency analysis showed that the V1, V3, and V4 are the most dominant V
635 families followed by V2 and V5 that had significantly lower frequencies. D family frequency
636 analysis showed that the D6, D3, D2 and D1 have the most prevalent representation, and J family
637 frequency showed that the J4, J5 and J6 have the most prevalent representation.

638 Next, we examined the distribution of the proteomically identified V-gene sequences to B cell
639 subsets (Figure 9B) and found that the V-genes predominantly map to mBC from D0 (46.83%),
640 followed by mBC from D10 (27.8%). Moreover, we found that 23.9% of V-genes map to D10
641 PB. Based on the dynamics of antibodies in serum (32), the majority of antibodies produced
642 following a boost challenge are the product of pre-existing mBC cells that were re-activated
643 following drug infusion, much like a response to a vaccine boost (23).

644 As mentioned above, flow cytometry of B cells following IFX administration allowed us to
645 identify a substantial increase in the frequency of PB at D10, which suggests that the B cell
646 dynamics following IFX infusion exhibits vaccine-like characteristics. Therefore, we expected to
647 find a majority of V-gene sequences mapping to IgG⁺ B cells that underwent class switch
648 recombination in the germinal center. Surprisingly, the majority of proteomically identified serum
649 antibodies were mapped to IgM⁺ B cells (Figure 9C).

650 Next, we aimed to provide support to the observation that *nt*ADA preferably use the λ light chain.
651 By quantifying the accumulative intensities of peptides derived from the constant region of both κ
652 and λ light chains, we calculated the ratio of κ : λ light chain in the elution fraction which comprise
653 both the *nt*ADA and *b*ADA (ADA-IgG), and in the flow through fraction that represent ADA-
654 depleted IgG (dep-IgG). The expected κ / λ ratio of IgG in human serum is 2 (66% κ and 33% λ).

655 Indeed, proteomic analysis of the dep-IgG (D0 and D10), resulted in an average κ/λ ratio of 2.1.
656 The same analysis of the ADA-IgG showed a significant shift of the κ/λ ratio to 1.19. The
657 proteomic analysis was carried out on samples from patient that exhibited a high neutralization
658 index (have high levels of *ntADA*) and designated ADA⁺ using AHLC (detects only ADA with
659 λ light chain). Brought together, this further suggests that *ntADA* contribute to shift in the $\kappa:\lambda$
660 light chain ratio.

661 Discussion

662 The use of therapeutic mAbs in treating a wide range of diseases and disorders is growing
663 exponentially. Nonetheless, a major shortcoming of their use is the development of ADA in
664 patients receiving the mAb. Advances in mAb engineering have enabled the development of fully
665 human mAbs with reduced immunogenicity without abolishing it completely. Thus a mAb
666 administered to a patient can still induce an immune sensitization as reflected by the production of
667 ADA, which is associated with low trough drug levels and can mediate loss of clinical response to
668 the drug (20).

669 The precise mechanism underlying ADA production is unknown, and many questions related to
670 its development remain unaddressed, including determining precise concentrations of ADA in
671 serum, which portion of the ADA exhibits neutralizing capacity, the immune pathway governing
672 the production of ADA, and ultimately, the molecular composition of ADA at the sequence level.
673 To address these questions, we chose the chimeric TNF α antagonist IFX as the model system.
674 First, we aimed to quantify the ADA level in patient sera. Many methods were previously
675 reported to evaluate serum ADA levels. These assays include radio-immunoassays (43), Biotin-
676 drug Extraction with Acid Dissociation (BEAD) (44), Precipitation and acid dissociation
677 (PANDA) (45), affinity capture elution ELISA (ACE) (46), and Homogenous Mobility Shift
678 Assay (HMSA) (47). While these assays are not limited to the λ light chain detection like the
679 AHLC assay, they provide mostly qualitative measures to assist physicians in deciding the most
680 appropriate intervention when treating patients, and many (if not all) studies underestimated
681 actual ADA levels (19). These assays also lack a standardization methodology that can enable the
682 comparison of ADA levels across health centers.

683 To provide quantitative measures describing the molecular landscape of ADA, we first developed
684 a bio-immunoassay that would allow quantify ADA levels based on the F(ab')₂ region of the mAb
685 because previous reports indicated that the ADA generated from mAb administration are mostly

686 anti-idiotypic (21). Indeed, the bio-immunoassay demonstrated higher sensitivity compared with
687 the AHLC assay used initially to detect ADA and was able to detect ADA when the AHLC assay
688 could not. Leveraging its improved sensitivity compared to the AHLC assay, we applied our
689 proprietary assay on sera from 54 patients treated with IFX and found that patients designated as
690 AHLC⁽⁺⁾ showed significantly higher levels of ADA (mean: 264 µg/ml) compared to the AHLC⁽⁻⁾
691 group (mean: 59.64 µg/ml). These results support the clinical use of AHLC assay because overall,
692 patients were correctly stratified leading to clinical decision-making that was based on a valid
693 indicative assay. Notwithstanding, the applicability of the AHLC assay, the newly developed
694 F(ab')₂-based bio-immunoassay demonstrated that ADA levels can reach extreme concentrations
695 that were not detected using the AHLC assay.

696 Some patients who develop ADA in response to IFX present a prolonged remission with
697 maintenance therapy despite repeated indications of high ADA and low IFX trough levels (20).
698 The mechanism of action of these ADA has significant influence on drug efficacy. For example,
699 *b*ADA are most likely to enhance the clearance of a drug whereas *nt*ADA will prevent a drug
700 from binding to its target. Hence, it is important to differentiate between *b*ADA and *nt*ADA, or in
701 other words, a need exists to identify sera with high levels of *nt*ADA that may predict the
702 likelihood of a patient losing a favorable response to an administered mAb. To achieve this, we
703 further revised our bio-immunoassay to qualitatively measure the neutralization index of ADA in
704 the serum of patients treated with IFX. Of note, as the neutralization index is a qualitative and not
705 a quantitative index, some patients may exhibit relatively low ADA levels and high neutralization
706 index. Using this assay on sera from the 46 ADA positive patients, revealed that patients who
707 tested positive utilizing the AHLC assay, exhibit a significantly higher neutralization index than
708 patients tested negatively for it (i.e., AHLC⁽⁻⁾). Noteworthy, the AHLC assay is based on the anti-
709 λ light chain antibody at the detection stage, suggesting that sera with high neutralization index
710 comprise ADA that preferably use the λ light chain (either *b*ADA or *nt*ADA). This phenomenon
711 received additional support from our proteomic analysis in which we compared the changes in the
712 ratio between peptides derived from κ and λ constant light chains from ADA-IgG pool and
713 peptide derived from depleted ADA IgG polyclonal pool (dep-IgG). This analysis demonstrated
714 that the κ/λ ratio in the total IgG compartment is as expected and is decreased in the mAb-specific
715 compartment (κ/λ ratio 2.1 and 1.19 for dep-IgG and ADA-IgG, respectively). The preferential
716 use of the λ light chain in neutralizing antibodies has been previously reported (21, 48), however,
717 the authors of those studies did not provide an explanation beyond the structural adaptability of

718 the light chain toward the target. The relevance of the reported cases showing λ chain bias is not
719 clear. Similar phenomena was reported in B-1 sub-population, unlike follicular B cells, B-1 cells
720 exhibit an increased frequency of lambda light chains (49). The recurrence of BCRs with the
721 enrichment of λ light chain has been considered to result from strong antigen-dependent selection
722 of the B-1 cell repertoire (50).

723 Repetitive administration of mAbs may induce a strong humoral response manifested in the
724 production of ADA. We hypothesized that mAb administration is similar to the response that
725 occurs following a boost vaccine. Others and we have demonstrated that boost vaccines induce a
726 strong proliferation of PB that can be detected in blood circulation several days after the boost.
727 The “wave” of B cells after the boost vaccine are dominated by antigen-specific B cell (34) thus,
728 repertoire analysis of these cells can provide invaluable data about the antigen-specific antibody
729 repertoires. Utilizing flow cytometry showed an order of magnitude increase in PB compartment
730 10 days after IFX infusion, suggesting that the immune response following IFX administration is
731 indeed similar to a vaccine response. To the best of our knowledge, this is the first report to
732 identify a vaccine like response following therapeutic mAb administration.

733 Next, we aimed to provide a comprehensive repertoire profile of the B cells induced after mAb
734 administration. To achieve this, we applied an “omics” approach as previously described (23, 26,
735 39) that is based on the integration of NGS of the V-genes and proteomic analysis of serum ADA.
736 NGS of V-genes revealed no bias in the V(D)J usage across isotypes, cell types, and time point.
737 These data suggest that the original repertoire that existed before mAb administration and
738 antigen-specific repertoire induced by IFX administration is formed by random recombination
739 processes without preferential use of any particular V(D)J segment. Comparative repertoire
740 analysis of the V-genes between time points (before and after IFX administration) revealed that
741 post-IFX administration, PB exhibit longer CDRH3 and lower SHM rates. Although the B cell
742 dynamics after mAb administration are similar to those that occur after a boost vaccine, the
743 repertoire measures show a different profile. It was previously reported that the antibodies
744 generated after a boost vaccine exhibit shorter CDRH3, high SHM (40-42).

745 To explain these data we revisited two reports: the first describes how the immune response in
746 TNF α -deficient mice was “diverted” to the marginal zone instead of to the germinal center (51)
747 and the characteristics of the immune response in the marginal zone is directly affected by low
748 levels of the AID that in turn is reflected in lower SHM rate. The second reported a skewed λ

749 chain usage in B-1 cells (49). Based on these reports we propose a mechanistic model according
750 to which administration of TNF α antagonist blocks the TNF α on one hand and induces a vaccine-
751 like response on the other. Due to the TNF α blockade, immune response of B cells occurs extra
752 follicular where AID is downregulated, thus the encoded ADA exhibit lower SHM rates.
753 Moreover, the data suggests that the immune response following mAb administration may be a T
754 cell independent (TI) response which is governed by the B-1 cell lineage with the characteristics
755 mentioned of an increased usage of λ light chains and little to non-evidence for SHM (49, 52).

756 Another possible mechanism that should be further explored is the strong TI immune response in
757 the marginal zone that is also induced by a drug/ADA immune-complex (IC). It was previously
758 suggested that many of the immune-mediated adverse effects attributed to ADA require the
759 formation of an IC intermediate that can have a variety of downstream effects (6, 53). In the
760 context of the system we investigated, administration of a TNF α antagonist will divert the
761 immune response extra follicular either by TNF α blockade or by the formation of an IC carrying
762 multiple mAbs that can induce the cross-linking of cognate BCR. The BCR of ADA-encoding B
763 cells will undergo co-clustering leading to their activation in the TI pathway.

764 Of note, insights from this study are restricted to the immune response following treatment with
765 TNF α antagonists, as it is specifically affected by the drug's mechanism of action. First, TNF α is
766 a trimer that has the propensity to form immunocomplexes with the drug. Second, blocking TNF α
767 “simulates” a scenario that was observed in TNF α knockout mice. Combined, these attributes
768 contribute to the specific nature of the immune response which is suggested to be diverted to the
769 extra follicular, TI immune response. Moreover, the deep analysis data was obtained from one
770 patient. However, this patient exhibited a set of attributes including high ADA level, high
771 neutralization index, low trough level and lack of immunosuppressant treatments. These attributes
772 enabled to generate insights that are directly relevant to the drug administration.

773 In our study we examined molecular aspects related to the formation of ADA. To the best of our
774 knowledge, this is the first report describing ADA repertoire that resulted in insights about a
775 possible mechanism of ADA formation. Further work will be needed to elucidate additional
776 phenotypic markers of the B cells induced by mAb administration and the role of IC in the
777 activation of the B cell. Moreover, the mechanism described here covers the response to a TNF α -
778 antagonist, and by using the same omics approaches, it will be highly informative to study the B
779 cell response following treatment with other mAbs that induce ADA formation. We envision that

780 high throughput data obtained from such studies can facilitate our understanding on why and how,
781 mAb administration generates ADA and eventually may contribute guidelines for engineering
782 therapeutic mAbs with reduced immunogenicity.

783 **Acknowledgments**

784 **General:** We are grateful to George Georgiou for assisting with the LC-MS/MS measurements at UT Austin, for
785 Ulrich von Pawel-Rammingen from the Department of Molecular Biology, Umea University who kindly donated the
786 plasmid with the gene encoding the IdeS.

787 This manuscript has been released as a Pre-Print at BioRxiv. DOI: <https://doi.org/10.1101/509489>

788 **Funding:** The work was partially supported by BSF grant 2017359 (Y.W.)

789 **Author contributions:** A.V.M, S.B.H, I.B. and Y.W. conceived the research. A.V.M. S.R. and Y.W. designed the
790 experiments, A.V.M., S.R., M.Y., E.F. and Y.D. performed experiments, A.V.M., S.R., S.B.H, M.Y., E.F., B.U. and
791 U.K. collected and processed clinical samples, A.V.M, A.K. and Y.W. carried out data analysis, A.V.M. and Y.W.
792 wrote the manuscript.

793 **Competing interests:** The authors declare no competing financial interests.

794

References

1. Grilo AL, Mantalaris A. The Increasingly Human and Profitable Monoclonal Antibody Market. *Trends in biotechnology* (2019) 37(1):9-16. doi: 10.1016/j.tibtech.2018.05.014.
2. van Schouwenburg PA, Rispens T, Wolbink GJ. Immunogenicity of anti-TNF biologic therapies for rheumatoid arthritis. *Nat Rev Rheumatol* (2013) 9(3):164-72. doi: 10.1038/nrrheum.2013.4.
3. De Groot AS, Scott DW. Immunogenicity of protein therapeutics. *Trends in immunology* (2007) 28(11):482-90. doi: 10.1016/j.it.2007.07.011.
4. Hansel TT, Kropshofer H, Singer T, Mitchell JA, George AJ. The safety and side effects of monoclonal antibodies. *Nat Rev Drug Discov* (2010) 9(4):325-38. doi: 10.1038/nrd3003.
5. Bloem K, Hernandez-Breijo B, Martinez-Feito A, Rispens T. Immunogenicity of Therapeutic Antibodies: Monitoring Antidrug Antibodies in a Clinical Context. *Ther Drug Monit* (2017) 39(4):327-32. doi: 10.1097/FTD.0000000000000404.
6. Krishna M, Nadler SG. Immunogenicity to Biotherapeutics - The Role of Anti-drug Immune Complexes. *Frontiers in Immunology* (2016) 7. doi: 10.3389/fimmu.2016.00021.
7. Nelson AL, Dhimolea E, Reichert JM. Development trends for human monoclonal antibody therapeutics. *Nat Rev Drug Discov* (2010) 9(10):767-74. doi: 10.1038/nrd3229.
8. Ben-Horin S, Heap GA, Ahmad T, Kim H, Kwon T, Chowers Y. The immunogenicity of biosimilar infliximab: can we extrapolate the data across indications? *Expert Rev Gastroenterol Hepatol* (2015) 9 Suppl 1:27-34. doi: 10.1586/17474124.2015.1091307.
9. Bendtzen K. Immunogenicity of Anti-TNF- α Biotherapies: II. Clinical Relevance of Methods Used for Anti-Drug Antibody Detection. *Frontiers in Immunology* (2015) 6:109. doi: 10.3389/fimmu.2015.00109.
10. Putnam WS, Prabhu S, Zheng Y, Subramanyam M, Wang Y-MC. Pharmacokinetic, pharmacodynamic and immunogenicity comparability assessment strategies for monoclonal antibodies. *Trends in biotechnology* (2010) 28(10):509-16. doi: 10.1016/j.tibtech.2010.07.001.
11. Sands BE, Anderson FH, Bernstein CN, Chey WY, Feagan BG, Fedorak RN, et al. Infliximab maintenance therapy for fistulizing Crohn's disease. *New England Journal of Medicine* (2004) 350(9):876-85. doi: 10.1056/NEJMoa030815.
12. Mitoma H, Horiuchi T, Hatta N, Tsukamoto H, Harashima S, Kikuchi Y, et al. Infliximab induces potent anti-inflammatory responses by outside-to-inside signals through transmembrane TNF-alpha. *Gastroenterology* (2005) 128(2):376-92.
13. Ben-Horin S, Vande Casteele N, Schreiber S, Lakatos PL. Biosimilars in Inflammatory Bowel Disease: Facts and Fears of Extrapolation. *Clin Gastroenterol Hepatol* (2016) 14(12):1685-96. doi: 10.1016/j.cgh.2016.05.023.
14. Baker MP, Reynolds HM, Lumicisi B, Bryson CJ. Immunogenicity of protein therapeutics: The key causes, consequences and challenges. *Self Nonself* (2010) 1(4):314-22. doi: 10.4161/self.1.4.13904.
15. Ungar B, Engel T, Yablecovitch D, Lahat A, Lang A, Avidan B, et al. Prospective Observational Evaluation of Time-Dependency of Adalimumab Immunogenicity and Drug Concentrations: The Poetic Study. *The American journal of gastroenterology* (2018) 113(6):890-8. doi: 10.1038/s41395-018-0073-0.
16. Ungar B, Chowers Y, Yavzori M, Picard O, Fudim E, Har-Noy O, et al. The temporal evolution of antidrug antibodies in patients with inflammatory bowel disease treated with infliximab. *Gut* (2014) 63(8):1258-64. doi: 10.1136/gutjnl-2013-305259.
17. Vincent FB, Morand EF, Murphy K, Mackay F, Mariette X, Marcelli C. Antidrug antibodies (ADAb) to tumour necrosis factor (TNF)-specific neutralising agents in chronic inflammatory diseases: a real issue, a clinical perspective. *Ann Rheum Dis* (2013) 72(2):165-78. doi: 10.1136/annrheumdis-2012-202545.

- 845 18. Tatarewicz S, Miller JM, Swanson SJ, Moxness MS. Rheumatoid factor interference in
846 immunogenicity assays for human monoclonal antibody therapeutics. *J Immunol Methods* (2010)
847 357(1-2):10-6. doi: 10.1016/j.jim.2010.03.012.
- 848 19. Bloem K, van Leeuwen A, Verbeek G, Nurmohamed MT, Wolbink GJ, van der Kleij D, et
849 al. Systematic comparison of drug-tolerant assays for anti-drug antibodies in a cohort of
850 adalimumab-treated rheumatoid arthritis patients. *J Immunol Methods* (2015) 418:29-38. doi:
851 10.1016/j.jim.2015.01.007.
- 852 20. Ben-Horin S, Chowers Y. Tailoring anti-TNF therapy in IBD: drug levels and disease
853 activity. *Nature reviews Gastroenterology & hepatology* (2014) 11(4):243-55. doi:
854 10.1038/nrgastro.2013.253.
- 855 21. Ben-Horin S, Yavzori M, Katz L, Kopylov U, Picard O, Fudim E, et al. The immunogenic
856 part of infliximab is the F(ab')₂, but measuring antibodies to the intact infliximab molecule is
857 more clinically useful. *Gut* (2010) 60(1):gut.2009.201533-48. doi: 10.1136/gut.2009.201533.
- 858 22. Wenig K, Chatwell L, von Pawel-Rammingen U, Björck L, Huber R, Sonderrmann P.
859 Structure of the streptococcal endopeptidase IdeS, a cysteine proteinase with strict specificity for
860 IgG. *Proceedings of the National Academy of Sciences of the United States of America* (2004)
861 101(50):17371-6. doi: 10.1073/pnas.0407965101.
- 862 23. Lavinder JJ, Wine Y, Giesecke C, Ippolito GC, Horton AP, Lungu OI, et al. Identification
863 and characterization of the constituent human serum antibodies elicited by vaccination.
864 *Proceedings of the National Academy of Sciences of the United States of America* (2014)
865 111(6):2259-64. doi: 10.1073/pnas.1317793111.
- 866 24. Menzel U, Greiff V, Khan TA, Haessler U, Hellmann I, Friedensohn S, et al.
867 Comprehensive Evaluation and Optimization of Amplicon Library Preparation Methods for High-
868 Throughput Antibody Sequencing. *PLOS ONE* (2014) 9(5). doi: 10.1371/journal.pone.0096727.
- 869 25. Avram O, Vaisman-Mentesh A, Yehezkel D, Ashkenazy H, Pupko T, Wine Y. ASAP, A
870 Webserver for Immunoglobulin-Sequencing Analysis Pipeline. *Frontiers in Immunology* (2018)
871 9. doi: 10.3389/fimmu.2018.01686.
- 872 26. Boutz DR, Horton AP, Wine Y, Lavinder JJ, Georgiou G, Marcotte EM. Proteomic
873 Identification of Monoclonal Antibodies from Serum. *Analytical Chemistry* (2014) 86(10):4758-
874 66. doi: 10.1021/ac4037679.
- 875 27. Cox J, Mann M. MaxQuant enables high peptide identification rates, individualized p.p.b.-
876 range mass accuracies and proteome-wide protein quantification. *Nature biotechnology* (2008)
877 26(12):1367-72. doi: 10.1038/nbt.1511.
- 878 28. Cox J, Hein MY, Lubner CA, Paron I, Nagaraj N, Mann M. Accurate proteome-wide label-
879 free quantification by delayed normalization and maximal peptide ratio extraction, termed
880 MaxLFQ. *Molecular & cellular proteomics : MCP* (2014) 13(9):2513-26. doi:
881 10.1074/mcp.M113.031591.
- 882 29. Cox J, Neuhauser N, Michalski A, Scheltema RA, Olsen JV, Mann M. Andromeda: a
883 peptide search engine integrated into the MaxQuant environment. *Journal of proteome research*
884 (2011) 10(4):1794-805. doi: 10.1021/pr101065j.
- 885 30. von Pawel-Rammingen U, Johansson BP, Björck L. IdeS, a novel streptococcal cysteine
886 proteinase with unique specificity for immunoglobulin G. *The EMBO Journal* (2002) 21(7):1607-
887 15. doi: 10.1093/emboj/21.7.1607.
- 888 31. Kopylov U, Mazor Y, Yavzori M, Fudim E, Katz L, Coscas D, et al. Clinical utility of
889 antihuman lambda chain-based enzyme-linked immunosorbent assay (ELISA) versus double
890 antigen ELISA for the detection of anti-infliximab antibodies. *Inflammatory bowel diseases*
891 (2012) 18(9):1628-33. doi: 10.1002/ibd.21919.
- 892 32. Lee J, Boutz DR, Chromikova V, Joyce MG, Vollmers C, Leung K, et al. Molecular-level
893 analysis of the serum antibody repertoire in young adults before and after seasonal influenza
894 vaccination. *Nature Medicine* (2016) 22(12):1456-+. doi: 10.1038/nm.4224.

- 895 33. Haney DJ, Lock MD, Gurwith M, Simon JK, Ishioka G, Cohen MB, et al.
896 Lipopolysaccharide-specific memory B cell responses to an attenuated live cholera vaccine are
897 associated with protection against *Vibrio cholerae* infection. *Vaccine* (2018) 36(20):2768-73.
- 898 34. Davydov AN, Obratsova AS, Lebedin MY, Turchaninova MA, Staroverov DB, Merzlyak
899 EM, et al. Comparative Analysis of B-Cell Receptor Repertoires Induced by Live Yellow Fever
900 Vaccine in Young and Middle-Age Donors. *Front Immunol* (2018) 9:2309. doi:
901 10.3389/fimmu.2018.02309.
- 902 35. Blanchard-Rohner G, Pulickal AS, der Zijde CMJ-v, Snape MD, Pollard AJ. Appearance
903 of peripheral blood plasma cells and memory B cells in a primary and secondary immune
904 response in humans. *Blood* (2009) 114(24):4998-5002. doi: 10.1182/blood-2009-03-211052.
- 905 36. Greiff V, Menzel U, Haessler U, Cook SC, Friedensohn S, Khan TA, et al. Quantitative
906 assessment of the robustness of next-generation sequencing of antibody variable gene repertoires
907 from immunized mice. *BMC immunology* (2014) 15(1):40. doi: 10.1186/s12865-014-0040-5.
- 908 37. Mroczek ES, Ippolito GC, Rogosch T, Hoi KH, Hwangpo TA, Brand MG, et al.
909 Differences in the composition of the human antibody repertoire by B cell subsets in the blood.
910 *Frontiers in immunology* (2014) 5:96-. doi: 10.3389/fimmu.2014.00096.
- 911 38. Volpe JM, Kepler TB. Large-scale analysis of human heavy chain V(D)J recombination
912 patterns. *Immunome research* (2008) 4:3-. doi: 10.1186/1745-7580-4-3.
- 913 39. Wine Y, Boutz DR, Lavinder JJ, Miklos AE, Hughes RA, Hoi KH, et al. Molecular
914 deconvolution of the monoclonal antibodies that comprise the polyclonal serum response. *Proc
915 Natl Acad Sci USA* (2013) 110(8):2993-8. doi: 10.1073/pnas.1213737110.
- 916 40. Ademokun A, Wu YC, Martin V, Mitra R, Sack U, Baxendale H, et al. Vaccination-
917 induced changes in human B-cell repertoire and pneumococcal IgM and IgA antibody at different
918 ages. *Aging cell* (2011) 10(6):922-30. doi: 10.1111/j.1474-9726.2011.00732.x.
- 919 41. Galson JD, Trück J, Fowler A, Clutterbuck EA, Münz M, Cerundolo V, et al. Analysis of
920 B Cell Repertoire Dynamics Following Hepatitis B Vaccination in Humans, and Enrichment of
921 Vaccine-specific Antibody Sequences. *EBioMedicine* (2015) 2(12):2070-9. doi:
922 <https://doi.org/10.1016/j.ebiom.2015.11.034>.
- 923 42. DeKosky BJ, Lungu OI, Park D, Johnson EL, Charab W, Chrysostomou C, et al. Large-
924 scale sequence and structural comparisons of human naive and antigen-experienced antibody
925 repertoires. *Proc Natl Acad Sci U S A* (2016) 113(19):E2636-45. doi: 10.1073/pnas.1525510113.
- 926 43. Svenson M, Geborek P, Saxne T, Bendtzen K. Monitoring patients treated with anti-TNF-
927 α biopharmaceuticals: assessing serum infliximab and anti-infliximab antibodies. *Rheumatology
928 (Oxford, England)* (2007) 46(12):1828-34. doi: 10.1093/rheumatology/kem261.
- 929 44. Lofgren JA, Wala I, Koren E, Swanson SJ, Jing S. Detection of neutralizing anti-
930 therapeutic protein antibodies in serum or plasma samples containing high levels of the
931 therapeutic protein. *Journal of Immunological Methods* (2006) 20(1-2):101-8.
- 932 45. Zoghbi J, Xu Y, Grabert R, Theobald V, Richards S. A breakthrough novel method to
933 resolve the drug and target interference problem in immunogenicity assays. *J Immunol Methods*
934 (2015) 426:62-9. doi: 10.1016/j.jim.2015.08.002.
- 935 46. Schmidt E, Hennig K, Mengede C, Zillikens D, Kromminga A. Immunogenicity of
936 rituximab in patients with severe pemphigus. *Clin Immunol* (2009) 132(3):334-41. doi:
937 10.1016/j.clim.2009.05.007.
- 938 47. Hernandez-Breijo B, Chaparro M, Cano-Martinez D, Guerra I, Iborra M, Cabriada JL, et
939 al. Standardization of the homogeneous mobility shift assay protocol for evaluation of anti-
940 infliximab antibodies. Application of the method to Crohn's disease patients treated with
941 infliximab. *Biochem Pharmacol* (2016) 122:33-41. doi: 10.1016/j.bcp.2016.09.019.
- 942 48. Robinson JE, Hastie KM, Cross RW, Yenni RE, Elliott DH, Rouelle JA, et al. Most
943 neutralizing human monoclonal antibodies target novel epitopes requiring both Lassa virus
944 glycoprotein subunits. *Nature communications* (2016) 7:11544-. doi: 10.1038/ncomms11544.

- 945 49. Hayakawa K, Hardy RR, Herzenberg LA. Peritoneal Ly-1 B cells: genetic control,
946 autoantibody production, increased lambda light chain expression. *Eur J Immunol* (1986)
947 16(4):450-6. doi: 10.1002/eji.1830160423.
- 948 50. Rowley B, Tang L, Shinton S, Hayakawa K, Hardy RR. Autoreactive B-1 B cells:
949 constraints on natural autoantibody B cell antigen receptors. *J Autoimmun* (2007) 29(4):236-45.
- 950 51. Pasparakis M, Alexopoulou L, Episkopou V, Kollias G. Immune and inflammatory
951 responses in TNF alpha-deficient mice: a critical requirement for TNF alpha in the formation of
952 primary B cell follicles, follicular dendritic cell networks and germinal centers, and in the
953 maturation of the humoral immune response. *Journal of Experimental Medicine* (1996)
954 184(4):1397-411. doi: 10.1084/jem.184.4.1397.
- 955 52. Kantor AB, Herzenberg LA. Origin of murine B cell lineages. *Annu Rev Immunol* (1993)
956 11:501-38. doi: 10.1146/annurev.iy.11.040193.002441.
- 957 53. Bar-Yoseph H, Pressman S, Blatt A, Vainberg SG, Maimon N, Starosvetsky E, et al.
958 Infliximab-Tumor Necrosis Factor Complexes Elicit Formation of Anti-drug Antibodies.
959 *Gastroenterology* (2019) In Press. doi: 10.1053/j.gastro.2019.08.009.
- 960

Figure legends

Figure 1: IFX digestion and IFX-F(ab')₂ purification. (A) Schematic representation of IgG digestion with IdeS. IdeS is a highly specific immunoglobulin-degrading enzyme that cleaves below the disulfide bonds in the IgG hinge region. The cleavage results in the production of IFX-F(ab')₂ fragment and two ½ Fc fragments. (B) SDS-PAGE analysis of intact IgG (lane 2), following IdeS digestion (lane 3) and purified IFX-F(ab')₂ following a 2-step affinity chromatography purification including protein A and kappa-select columns (lane 4). (C) Presence of Fc and intact IgG traces was measured by direct ELISA where intact IFX and purified IFX-F(ab')₂ were compared to a control antigen (streptavidin) as coating agents followed by direct incubation with an anti-Fc HRP conjugate at the detection phase. (D) The functionality of the recovered IFX-F(ab')₂ was confirmed by testing it for TNF α binding by ELISA in comparison to intact IFX. The ELISA setup included TNF α as the coating agent and anti-K HRP conjugate at the detection phase. For panel C–D, triplicate averages were calculated as mean, with error bars indicating s.d.

Figure 2: Standard curve for ADA quantification in patients treated with IFX. ADA were purified from sera of 17 patients treated with IFX, utilizing consecutive affinity chromatography steps including protein G and custom made IFX-F(ab')₂ columns. (A) Purified ADA were tested in ELISA for functionality. TNF α was used as the coating agent followed by incubation with purified ADA and anti-Fc HRP conjugate at the detection phase. Control included serum obtained from a healthy donor. (B) SDS-PAGE analysis of intact IFX (lane 2) and purified ADA (lane 3). (C) The effect of serum on ADA standard was tested in ELISA by spiking-in differential concentrations of ADA into ADA negative serum.

Figure 3: AHLC and the newly developed mAb-F(ab')₂ based bio-immunoassay configuration and their application on serum samples from patients treated with IFX. (A) AHLC assay is based on an ELISA where TNF α is used as the coating agent, following the incubation with the mAb drug followed by serial dilutions of the tested sera. anti- λ HRP conjugate is used at the detection phase. (B) The newly developed mAb-F(ab')₂ based bio-immunoassay configuration. The assay is based on an ELISA where mAb-F(ab')₂ is used as the coating agent followed by serial dilutions of the tested sera. Anti-Fc HRP conjugate is used at the detection phase. (C) ELISA obtained by utilizing the AHLC assay on two serum samples. Using this assay, one of the tested sera showed detectable levels of ADA (AHLC⁽⁺⁾) and one had no detectable levels of ADA (AHLC⁽⁻⁾). (D) Both serum samples were tested by the newly developed mAb-F(ab')₂ based bio-immunoassay. This assay was able to detect ADA in both sera. For C–D, averages were calculated as mean from triplicates, with error bars indicating s.d.

Figure 4: Configuration of the assay for determining the neutralization index of ADA in patient sera and competitive ELISA between ADA and rhTNF α . (A) The newly developed mAb-F(ab')₂ based bio-immunoassay configuration (left) and the modified configuration where mAb-F(ab')₂ binding site is blocked by saturating the assay with rhTNF α (right). (B) Competitive effect of rhTNF α on ADA binding to IFX-F(ab')₂. ELISA plate was coated with 5 μ g/ml of IFX-F(ab')₂. ADA standard was diluted 3-fold in blocking solution supplemented with 5nM rhTNF α . ADA diluted 3-fold in blocking solution without the presence of rhTNF α served as a control.

Figure 5: Neutralization index ELISA. (A) Graph representing the ELISA results obtained utilizing the neutralization assay on serum that was designated as AHLC⁽⁻⁾ and (B) AHLC⁽⁺⁾. In both (A) and (B) the effect of soluble TNF α on ADA detection was evaluated and neutralization index was determined. (C) Scatter plot consolidating the neutralization index obtained by applying the immunoassay on sera from 46 ADA positive patients treated with IFX (**** $P < 0.0001$, Mann-Whitney U test). For A–C, averages were calculated as mean, with error bars indicating s.d.

Figure 6: V, D and J family usage in B cell following IFX infusion. mBC and PB from a patient treated with IFX were collected at two time points (D0, D10) and processed for NGS analysis. The V family usage showed no difference between D0 and D10, different B cell subsets and isotypes. The D and J family usage showed no difference between time points.

Figure 7: CDRH3 length at two time point and across isotypes. PB from a patient treated with IFX were collected at two time points (D0, D10) and processed for NGS analysis. An increase in antibody CDRH3 length was observed. (*** $P < 0.001$, Mann-Whitney U test).

Figure 8: Somatic hyper mutations. PB from a patient treated with IFX were collected at two time points (D0, D10) and processed for NGS analysis. A decrease in the number of Ka mutations (number of non-synonymous mutation per codon) and Ks mutations (number of synonymous mutations per codon) was observed at D10. (**** $P < 0.0001$, Mann-Whitney U test).

1020 **Figure 9: V-gene and circulating antibody repertoire characteristics.** (A) The V(D)J family usage of V-gene
 1021 sequences that were identified by LC-MS/MS. (B) Mapping of V-gene sequences to B cell subsets and (C) isotypes,
 1022 based on NGS data.
 1023

1024 **Table 1: ADA concentrations in 55 serum samples from patients treated with IFX.** Serum samples were initially
 1025 stratified into AHLC (+) and AHLC (-) based on the AHLC assay used in the clinic. The newly developed bio-
 1026 immunoassay for the quantification of total ADA was applied on all serum samples and concentration are listed. All
 1027 ADA concentrations are in µg/ml.
 1028

AHLC ⁽⁻⁾ patients			AHLC ⁽⁺⁾ patients		
Patient #	AHLC µg/ml	New bio-immunoassay µg/ml	Patient #	AHLC µg/ml	New bio-immunoassay µg/ml
5645	0	867.33	14655	7.9	121.95
5557	0.9	0	15046	16.6	85.24
5381	1.9	0	15460	21.1	147.89
6497	1.6	26.26	15809	22.8	996.84
6386	1.7	0	15107	6.3	126.5
6259	0.8	41.39	14408	4.8	90.54
6098	1.3	0	4297	8.9	274.6
5993	1.3	0	5048	5.6	49.28
5882	1.7	152.72	5735	6.9	99.67
5822	1.3	0	6393	3.4	289.31
6291	0.7	19.43	6324	6.7	91.14
6616	0.3	84.05	6275	31.8	242.03
7083	1	97.29	6261	27.2	245.52
7041	1	0	6208	5.8	65.35
7004	0.7	4.28	6165	3	2.7
6866	1.3	80.05	6148	7.2	148.88
6788	1.8	46.83	9348	42.2	285.05
6740	1.5	0	8970	59.3	1268.5
14735	0.4	1.86	8816	27.2	396.2
14752	1.2	43.87	7553	46.7	178.83
14879	1.7	1.94	12113	20.9	772.83
14834	0.57	1.96	12104	20.9	441.09
13741	1.3	18	6329	11	87.31
13711	0.3	1.89	8178	7.9	55.11
14278	1.72	1.82	7653	16.1	53.52
			8856	42.4	87.97
			9454	7.8	265.35
			12343	16.5	358.54
			12345	37	329.49

1029
 1030
 1031
 1032
 1033
 1034

1035 **Table 2: B cell frequency of a patient treated with IFX.**

Time point	B cell subset	% Frequency of sorted cells (out of CD19+ cells)	No. of raw paired-end sequencing reads		No. of filtered paired-end sequencing reads			No. of unique IGH clonotypes extracted (Unique CDRH3)
			Replicate A	Replicate B	Replicate A	Replicate B	Joint	
D0	PB	0.9%	39,129	63,168	12,863	19,082	2041	1294
	mBC	10%	714,722	639,984	121,998	111,373	30,725	9146
D10	PB	11.5%	167,859	151,849	49,762	46,192	10,341	5590
	mBC	9.7%	528,765	488,619	143,864	133,879	40,899	19,521

1036
1037
1038
1039
1040

Table 3: Summary of identified peptides and the corresponding clonotype and antibody somatic variances in the LC-MS/MS spectra. E: elution, FT: flow-through.

	Day 0	Day 10
Total peptides	908	3177
Total antibody peptides	761	2805
Total CDRH3	42	224
Present in ≥ 2 technical replicates	30	166
Frequency ratio E/FT > 5	11	81
N ^o of clones	5	62
N ^o of somatic variances	35	205

1041

Figures

Figure 1

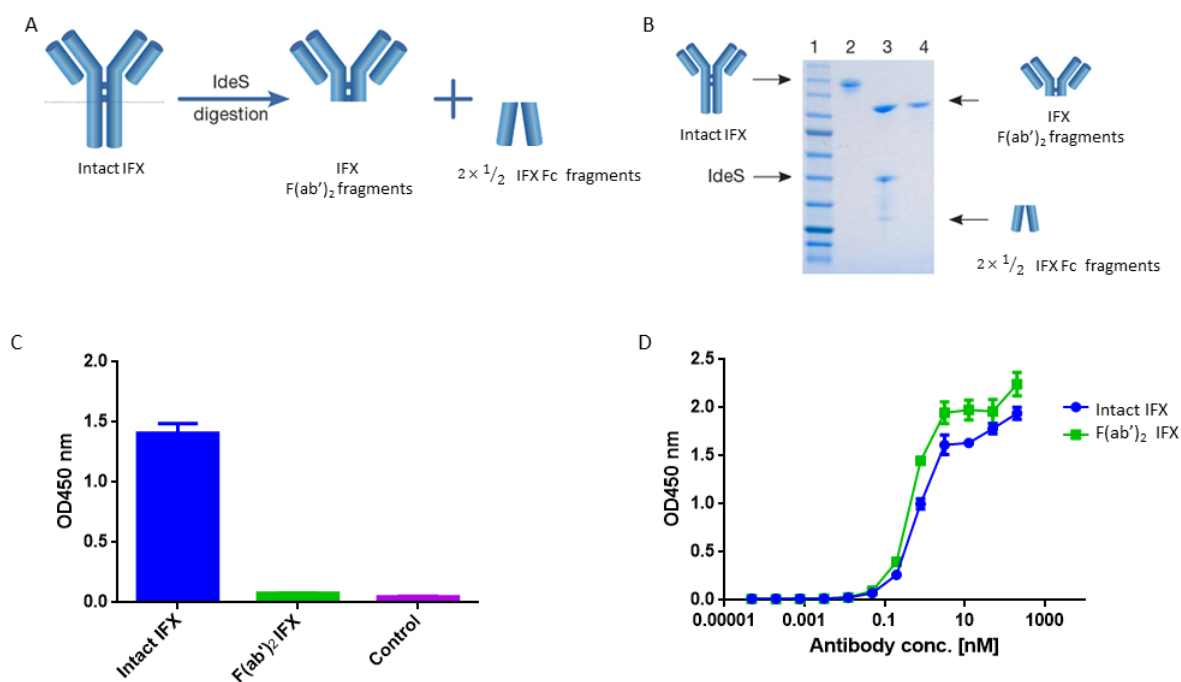


Figure 2

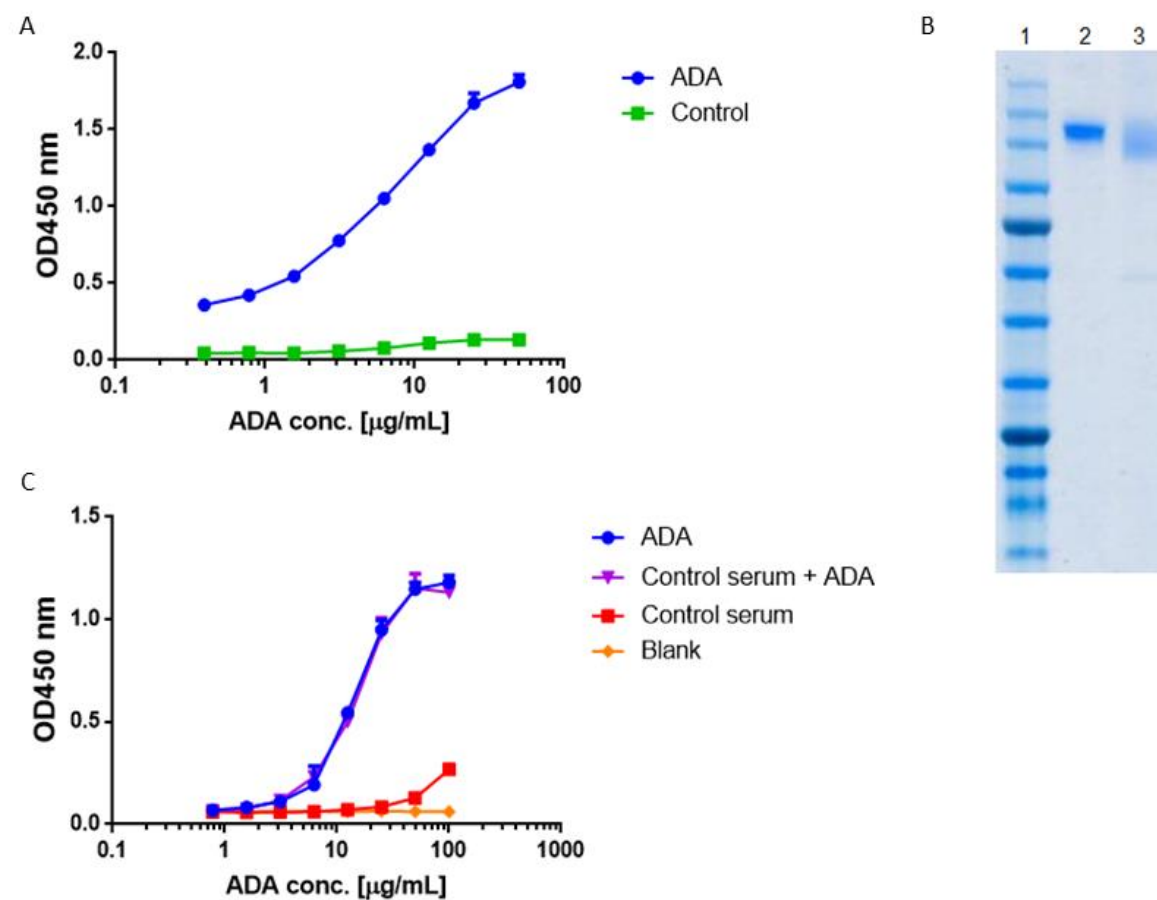


Figure 3

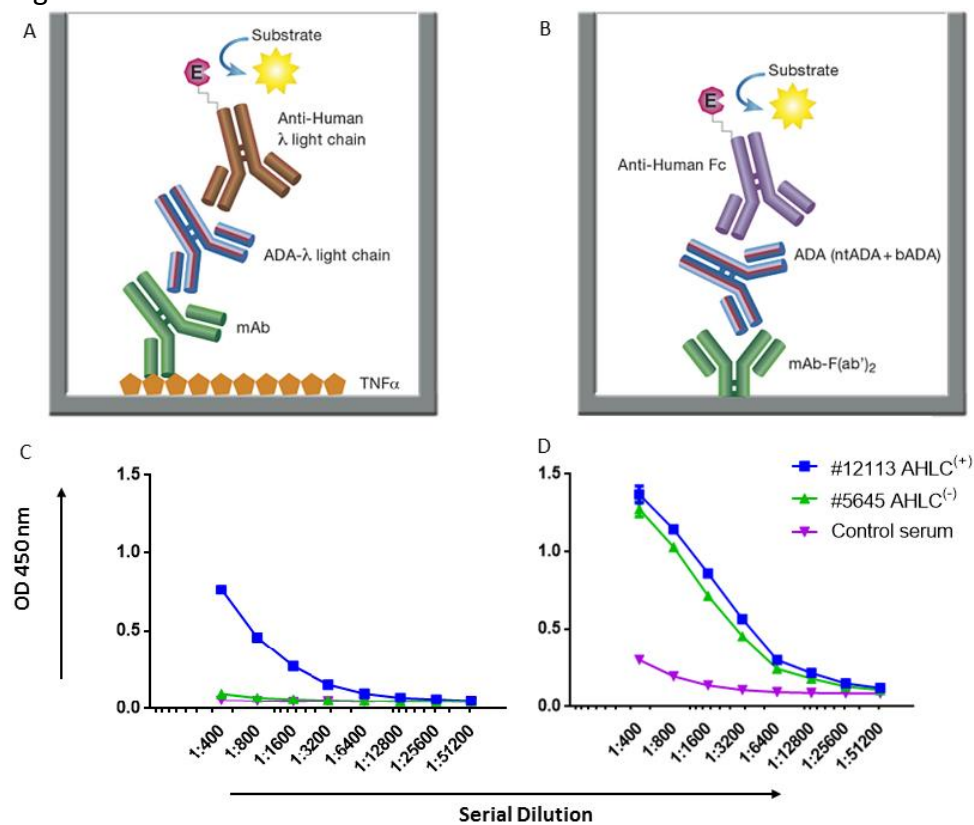


Figure 4

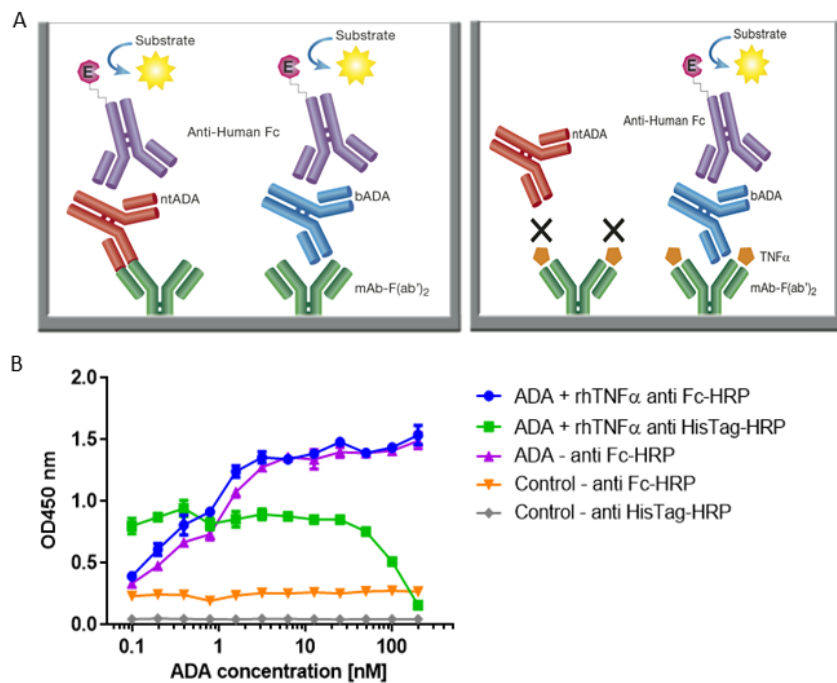


Figure 5

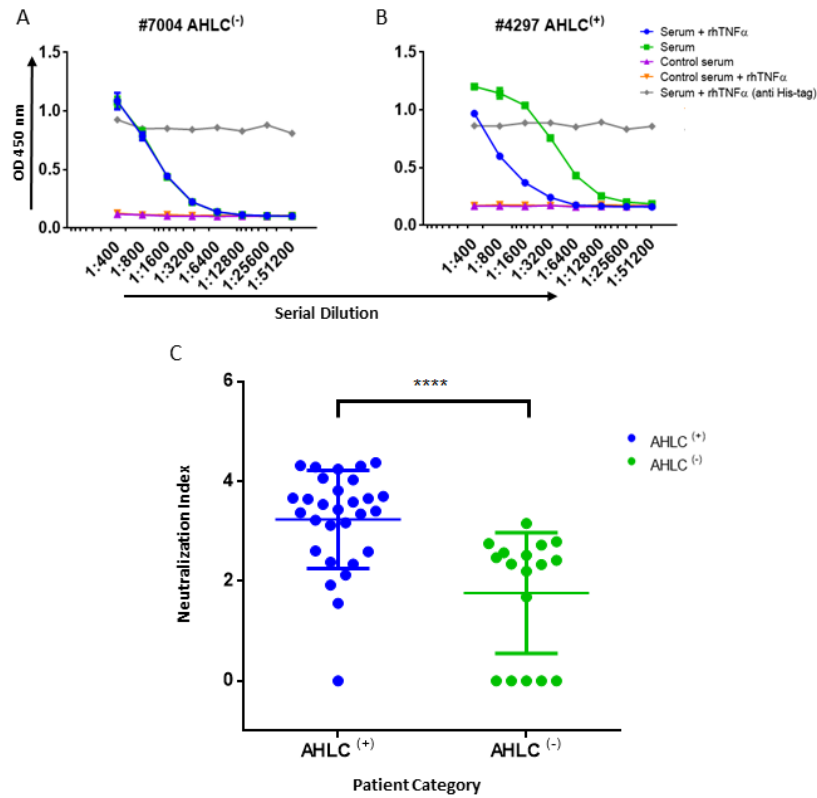


Figure 6

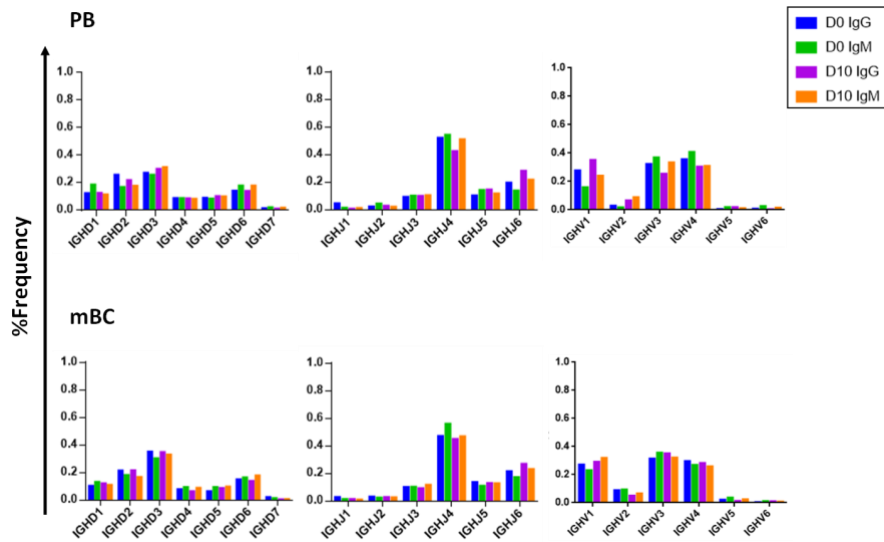


Figure 7

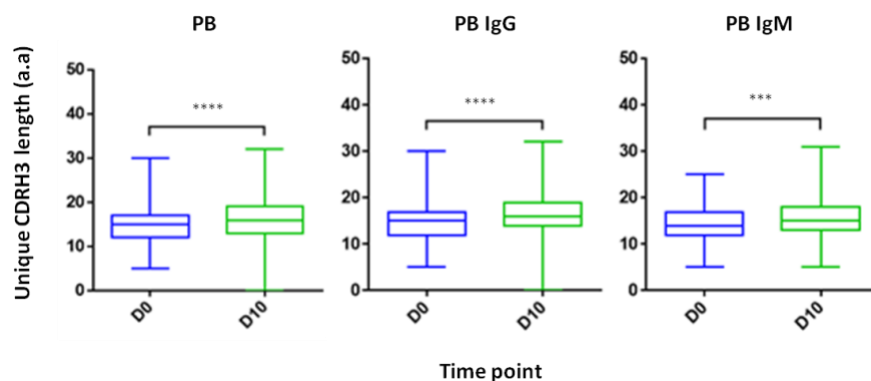


Figure 8

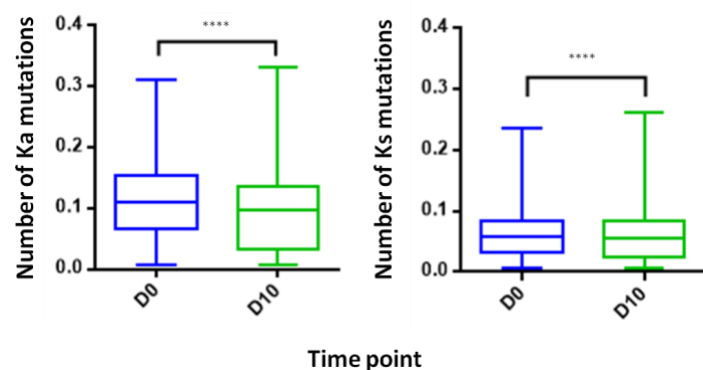


Figure 9

